

**Shock Compression of Metal Crystals: A
Comparison of Eulerian and Lagrangian
Elastic-Plastic Theories**

by JD Clayton

ARL-RP-0513

November 2014

Reprinted from the *International Journal of Applied Mechanics*. 2014;6(5):1450048-1-29.
DOI: 10.1142/S1758825114500483.

NOTICES

Disclaimers

The findings in this report are not to be construed as an official Department of the Army position unless so designated by other authorized documents.

Citation of manufacturer's or trade names does not constitute an official endorsement or approval of the use thereof.

Destroy this report when it is no longer needed. Do not return it to the originator.

Army Research Laboratory

Aberdeen Proving Ground, MD 21005-5069

ARL-RP-0513

November 2014

Shock Compression of Metal Crystals: A Comparison of Eulerian and Lagrangian Elastic-Plastic Theories

JD Clayton

Weapons and Materials Research Directorate, ARL

Reprinted from the *International Journal of Applied Mechanics*. 2014;6(5):1450048-1-29.
DOI: 10.1142/S1758825114500483.

REPORT DOCUMENTATION PAGE			<i>Form Approved</i> OMB No. 0704-0188		
Public reporting burden for this collection of information is estimated to average 1 hour per response, including the time for reviewing instructions, searching existing data sources, gathering and maintaining the data needed, and completing and reviewing the collection information. Send comments regarding this burden estimate or any other aspect of this collection of information, including suggestions for reducing the burden, to Department of Defense, Washington Headquarters Services, Directorate for Information Operations and Reports (0704-0188), 1215 Jefferson Davis Highway, Suite 1204, Arlington, VA 22202-4302. Respondents should be aware that notwithstanding any other provision of law, no person shall be subject to any penalty for failing to comply with a collection of information if it does not display a currently valid OMB control number. PLEASE DO NOT RETURN YOUR FORM TO THE ABOVE ADDRESS.					
1. REPORT DATE (DD-MM-YYYY) November 2014		2. REPORT TYPE Reprint		3. DATES COVERED (From - To) October 2012–October 2014	
4. TITLE AND SUBTITLE Shock Compression of Metal Crystals: A Comparison of Eulerian and Lagrangian Elastic-Plastic Theories			5a. CONTRACT NUMBER		
			5b. GRANT NUMBER		
			5c. PROGRAM ELEMENT NUMBER		
6. AUTHOR(S) JD Clayton			5d. PROJECT NUMBER DRI13-WMR-019		
			5e. TASK NUMBER		
			5f. WORK UNIT NUMBER		
7. PERFORMING ORGANIZATION NAME(S) AND ADDRESS(ES) U.S. Army Research Laboratory ATTN: RDRL-WMP-C Aberdeen Proving Ground, MD 21005-5069			8. PERFORMING ORGANIZATION REPORT NUMBER ARL-RP-0513		
9. SPONSORING/MONITORING AGENCY NAME(S) AND ADDRESS(ES)			10. SPONSOR/MONITOR'S ACRONYM(S)		
			11. SPONSOR/MONITOR'S REPORT NUMBER(S)		
12. DISTRIBUTION/AVAILABILITY STATEMENT Approved for public release; distribution is unlimited.					
13. SUPPLEMENTARY NOTES Reprinted from the International Journal of Applied Mechanics. 2014;6(5):1450048-1–29. DOI: 10.1142/S1758825114500483.					
14. ABSTRACT An unconventional nonlinear elastic theory is advocated for solids undergoing large compression as may occur in shock loading. This theory incorporates an Eulerian strain measure, in locally unstressed material coordinates. Analytical predictions of this theory and conventional Lagrangian theory for elastic shock stress in anisotropic single crystals of aluminum, copper and magnesium are compared. Eulerian solutions demonstrate greater accuracy compared to atomic simulation (aluminum) and faster convergence with increasing order of elastic constants entering the internal energy. A thermomechanical framework incorporating this Eulerian strain and accounting for elastic and plastic deformations is outlined in parallel with equations for Lagrangian finite strain crystal plasticity. For several symmetric crystal orientations, predicted values of volumetric compression at the Hugoniot elastic limit of the two theories begin to differ substantially when octahedral or prismatic slip system strengths exceed about 1% of the shear modulus. Predicted pressures differ substantially for volumetric compression in excess of 5%. Predictions of Eulerian theory are closer to experimental shock data for aluminum, copper, and magnesium polycrystals.					
15. SUBJECT TERMS elasticity, plasticity, shock physics, crystals, metals					
16. SECURITY CLASSIFICATION OF:			17. LIMITATION OF ABSTRACT UU	18. NUMBER OF PAGES 34	19a. NAME OF RESPONSIBLE PERSON JD Clayton
a. REPORT Unclassified	b. ABSTRACT Unclassified	c. THIS PAGE Unclassified			19b. TELEPHONE NUMBER (Include area code) 410-278-6146

SHOCK COMPRESSION OF METAL CRYSTALS: A COMPARISON OF EULERIAN AND LAGRANGIAN ELASTIC-PLASTIC THEORIES

J. D. CLAYTON

*Impact Physics, US Army Research Laboratory, RDRL-WMP-C
Aberdeen Proving Ground, MD 21005-5066, USA
jclayton@arl.army.mil*

Received 5 September 2013

Revised 13 June 2014

Accepted 28 July 2014

Published 17 October 2014

An unconventional nonlinear elastic theory is advocated for solids undergoing large compression as may occur in shock loading. This theory incorporates an Eulerian strain measure, in locally unstressed material coordinates. Analytical predictions of this theory and conventional Lagrangian theory for elastic shock stress in anisotropic single crystals of aluminum, copper and magnesium are compared. Eulerian solutions demonstrate greater accuracy compared to atomic simulation (aluminum) and faster convergence with increasing order of elastic constants entering the internal energy. A thermomechanical framework incorporating this Eulerian strain and accounting for elastic and plastic deformations is outlined in parallel with equations for Lagrangian finite strain crystal plasticity. For several symmetric crystal orientations, predicted values of volumetric compression at the Hugoniot elastic limit of the two theories begin to differ substantially when octahedral or prismatic slip system strengths exceed about 1% of the shear modulus. Predicted pressures differ substantially for volumetric compression in excess of 5%. Predictions of Eulerian theory are closer to experimental shock data for aluminum, copper, and magnesium polycrystals.

Keywords: Elasticity; plasticity; shock physics; crystals; metals.

1. Introduction

Nonlinear elastic constitutive models are needed if strains or rotations are large in anisotropic materials, or if the stress–strain response of the material is sufficiently nonlinear. Thermodynamic potentials of usual Lagrangian theories of nonlinear elasticity of crystals [Wallace, 1972; Thurston, 1974; Teodosiu, 1982; Clayton, 2011] incorporate the right Cauchy–Green strain tensor \mathbf{E} , a function of the (elastic) deformation gradient and its transpose. Such theories have been used with some success for describing high rate behavior of ceramics and minerals [Winey and Gupta, 2004; Clayton, 2009, 2010; Foulk and Vogler, 2010], metals [Clayton, 2005; Winey and Gupta, 2006; Vogler and Clayton, 2008], and concrete [Clayton, 2008],

to compressive strains of up to several percent or more. Another recent model for dynamic deformation of cubic single crystals incorporates the deviatoric part of the elastic Green strain for the elastic shear response coupled with a pressure–volume–temperature equation-of-state (EOS) [Luscher *et al.*, 2013] for the pressure. For isotropic (e.g., untextured polycrystalline) solids, nonlinear elasticity incorporating the logarithm of the left stretch (Hencky’s tensor) has been found accurate for a number of materials subjected to moderately large strains [Anand, 1979].

In the present work, alternative theory is advanced incorporating an unconventional Eulerian strain measure \mathbf{D} , with components referred to locally relaxed material coordinates, that is a function of the inverse elastic deformation gradient and its transpose. This strain, which has historically shown promise for hydrostatic compression [Davies, 1974; Weaver, 1976; Perrin and Delannoy, 1978], is applied in this work to problems involving simultaneous volume change and shear, i.e., shock compression. Herein, the designation “Eulerian” is used to refer to a strain that is a function of the inverse deformation gradient [Davies, 1974; Weaver, 1976; Nielsen, 1986], and not necessarily one referred to spatial coordinates. Strain tensor \mathbf{D} [defined formally in Eq. (2.3)] is thus Eulerian but referred to material coordinates, the latter feature enabling its use in constitutive models of anisotropic solids. In contrast, the Almansi strain tensor \mathbf{e} entering Murnaghan’s theory for isotropic solids [Murnaghan, 1937] is simultaneously Eulerian and referred to spatial coordinates, as is Hencky’s strain measure [Anand, 1979].

In recent work [Clayton, 2013], a complete thermoelastic theory incorporating \mathbf{D} was developed in parallel with Lagrangian \mathbf{E} -based theory, and analytical solutions to the one-dimensional (planar) shock problem were derived. Predictions of these solutions were compared for single crystals of quartz, sapphire, and diamond shocked in pure mode directions.^a These specific results did not demonstrate a clear advantage of one formulation over the other, and elastic constants of order three (sapphire) and order four (quartz and diamond) were needed to match Hugoniot data. On the other hand, analytical solutions for hydrostatic compression, uniaxial compression, and simple shear of generic cubic crystals with Cauchy symmetry and a characteristic pressure derivative of the ambient bulk modulus of four demonstrated certain advantages of Eulerian theory over Lagrangian theory in terms of general accuracy and intrinsic stability [Clayton, 2013].

In Sec. 2.3, this thermoelastic theory is newly applied to analyze shock compression of metals. Since the experimental Hugoniot elastic limit (HEL) usually occurs at small uniaxial compressive strain in ductile metals, purely elastic predictions of material strength that omit relaxation due to slip and/or twinning are idealizations when deformations are finite, though large elastic deformation in the absence of slip

^aDirections for purely longitudinal shock propagation were normal to X - and Z -cut faces in quartz and sapphire and normal to an X -cut face diamond; in that analysis of Y -cut quartz, transverse particle motion was neglected.

may be possible for small volumes of material or near defect cores [Teodosiu, 1982; Clayton *et al.*, 2014]. Apart from purely theoretical interest, application of analytical thermoelastic solutions to metals is useful for comparison with or validation of molecular dynamics simulations or their interatomic potentials [Zimmerman *et al.*, 2011], since defect-free configurations can be shocked to finite strains in simulations of small volumes over short time scales in such controlled simulations. Results are reported here for aluminum, copper and magnesium.

Crystal plasticity theory is generally needed for accurate continuum modeling of strength of single crystals shocked above their HEL. In Sec. 3.1, a thermomechanical framework accounting for finite elastic and plastic deformations is formulated, incorporating Eulerian elastic strain \mathbf{D} . For purposes of comparison, corresponding equations for Lagrangian theory incorporating strain tensor \mathbf{E} are also reported. Analytical results are available for isentropic compression of symmetric orientations of single crystals described by linear, rate-independent crystal plasticity [Johnson, 1972; Johnson, 1974], but these exclude geometric and material nonlinearities and thermal effects. Finite strain analytical solutions are not available for crystals with anisotropic inelasticity, and analysis of nonlinear elastic–plastic shock behavior can be complex even for isotropic solids [Germain and Lee, 1973; Wallace, 1980]. In Sec. 3.2, predictions of yield behavior (resolved shear stresses on common slip systems) and temperature rise under shock compression are compared for generic solids with properties representative of metallic crystals, in order to quantify strain regimes wherein the choice of nonlinear elastic model becomes important. Predictions of the pressure–volume EOS obtained from Eulerian and Lagrangian theories are compared with shock data [Marsh, 1980], demonstrating greater accuracy of the former at high pressures if material strength can be neglected.

2. Nonlinear Elasticity

Section 2.1 reviews continuum elasticity theory incorporating Lagrangian and Eulerian strain measures. Section 2.2 presents analytical solutions for steady, planar elastic shock propagation obtained from each theory. Only essential aspects are reported here since complete derivations have been recently presented elsewhere [Clayton, 2013]. Section 2.3 newly applies these solutions to single crystalline aluminum, copper, and magnesium.

2.1. Continuum thermoelasticity

Letting t denote time, spatial and initial material coordinates are related by the motion

$$\mathbf{x} = \mathbf{x}(\mathbf{X}, t). \quad (2.1)$$

The deformation gradient \mathbf{F} and volume ratio J are

$$\mathbf{F} = \partial \mathbf{x} / \partial \mathbf{X} = \nabla_0 \mathbf{x}, \quad J = \det \mathbf{F} > 0. \quad (2.2)$$

Lagrangian (\mathbf{E}) and Eulerian (\mathbf{D}) strain tensors, each with components referred to a Cartesian reference coordinate system, are defined by

$$\mathbf{E} = \frac{1}{2}(\mathbf{F}^T \mathbf{F} - \mathbf{1}), \quad \mathbf{D} = \frac{1}{2}(\mathbf{1} - \mathbf{F}^{-1} \mathbf{F}^{-T}). \quad (2.3)$$

Like \mathbf{E} , tensor \mathbf{D} is invariant under spatial rotation, and it differs from Almansi strain $\mathbf{e} = \frac{1}{2}(\mathbf{1} - \mathbf{F}^{-T} \mathbf{F}^{-1})$ of Murnaghan's theory [Murnaghan, 1937] that is not rotationally invariant and is thus restricted (with regards to use as a thermodynamic state variable) to isotropic elasticity. In the smooth case, local momentum and energy balances are, for no body forces or heat transfer

$$\nabla \cdot \boldsymbol{\sigma} = \rho \dot{\mathbf{v}}, \quad \boldsymbol{\sigma} = \boldsymbol{\sigma}^T, \quad \dot{U} = J \boldsymbol{\sigma} : \nabla \mathbf{v}. \quad (2.4)$$

Cauchy stress is $\boldsymbol{\sigma}$, internal energy per unit reference volume is U , particle velocity is \mathbf{v} , and spatial mass density is $\rho = \rho_0/J$. Denote by $\Psi = U - \theta\eta$ the Helmholtz free energy density, with θ and η denoting temperature and entropy. Thermodynamic potentials for Lagrangian and Eulerian theories are, respectively

$$U = \bar{U}(\mathbf{E}, \eta), \quad U = \hat{U}(\mathbf{D}, \eta); \quad \Psi = \bar{\Psi}(\mathbf{E}, \theta), \quad \Psi = \hat{\Psi}(\mathbf{D}, \theta). \quad (2.5)$$

For description of anisotropic elasticity in crystals, strain energy potentials associated with (2.5) are typically expanded as Taylor polynomials in strain tensors \mathbf{E} (Lagrangian) or \mathbf{D} (Eulerian), with the order of the polynomial corresponding to the maximum order of elastic constant present in the representation (e.g., a third-order polynomial incorporates elastic constants of up to order three). As explained in the Appendix, with increasing order such polynomials should ultimately converge to the same value of energy at a given strain of effective magnitude less than unity. Differences between predictions of Lagrangian and Eulerian representations in (2.5) result from truncation of their Taylor polynomials at a certain order.

Thermoelastic constitutive equalities and temperature change given by the local energy balance are derived using standard principles [Clayton, 2013]. For Lagrangian and Eulerian theory, these are, respectively

$$\begin{aligned} \bar{\mathbf{S}} &= \partial \bar{U} / \partial \mathbf{E} = \partial \bar{\Psi} / \partial \mathbf{E} = J \mathbf{F}^{-1} \boldsymbol{\sigma} \mathbf{F}^{-T}, \quad \theta = \partial \bar{U} / \partial \eta, \\ \eta &= -\partial \bar{\Psi} / \partial \theta; \quad \bar{c} \dot{\theta} = \theta \frac{\partial \bar{\mathbf{S}}}{\partial \theta} : \dot{\mathbf{E}}, \end{aligned} \quad (2.6)$$

$$\begin{aligned} \hat{\mathbf{S}} &= \partial \hat{U} / \partial \mathbf{D} = \partial \hat{\Psi} / \partial \mathbf{D} = J \mathbf{F}^T \boldsymbol{\sigma} \mathbf{F}, \quad \theta = \partial \hat{U} / \partial \eta, \\ \eta &= -\partial \hat{\Psi} / \partial \theta; \quad \hat{c} \dot{\theta} = \theta \frac{\partial \hat{\mathbf{S}}}{\partial \theta} : \dot{\mathbf{D}}. \end{aligned} \quad (2.7)$$

Specific heats per unit reference volume at fixed strain are $\bar{c} = \partial\bar{U}/\partial\theta$ and $\hat{c} = \partial\hat{U}/\partial\theta$.

As noted by Davies [1973], Eulerian strain tensor \mathbf{D} was perhaps first introduced by Thomsen [1972] for studying compression of cubic crystals. For cubic or isotropic solids subjected to spherical deformation of the form $\mathbf{F} = J^{1/3}\mathbf{1}$, stress $\sigma = -p\mathbf{1}$ is hydrostatic with p the Cauchy pressure. Under these (isentropic) conditions, as outlined in the Appendix, Lagrangian and Eulerian theories with internal energy functions (2.5)₁ expanded as third-order Taylor polynomials in \mathbf{E} and \mathbf{D} , respectively, yield the following respective pressure–volume equations-of-state:

$$p = -\partial\bar{U}/\partial J = \frac{3}{2}\mathbf{B}_0(J^{-1/3} - J^{1/3}) \left[1 - \frac{3}{4}\mathbf{B}'_0(J^{2/3} - 1) \right], \quad (2.8)$$

$$p = -\partial\hat{U}/\partial J = \frac{3}{2}\mathbf{B}_0(J^{-7/3} - J^{-5/3}) \left[1 + \frac{3}{4}(\mathbf{B}'_0 - 4)(J^{-2/3} - 1) \right], \quad (2.9)$$

where \mathbf{B}_0 and \mathbf{B}'_0 are the isentropic bulk modulus and its pressure derivative in the reference state. Equation (2.9) is identical to the two-parameter Birch–Murnaghan EOS [Birch, 1947; Thomsen, 1970]. As noted in the Appendix, differences in pressures predicted by (2.8) and (2.9) at the same volume ratio J arise from truncation of the associated internal energy functions at order three in either finite strain measure. Such differences would presumably eventually disappear with the addition of a sufficient number of higher-order terms involving higher-order derivatives \mathbf{B}''_0 etc. [Birch, 1978].

2.2. Analysis of planar shock compression

A steady planar shock with natural velocity \mathcal{D} moving through an unstressed solid can be described by the Rankine–Hugoniot equations [Germain and Lee, 1973; Thurston, 1974]

$$\mathcal{D} = v/(1 - J), \quad P = \rho_0\mathcal{D}v, \quad \llbracket U \rrbracket = \frac{1}{2}\rho_0v^2. \quad (2.10)$$

Particle velocity is v and axial shock stress is P , positive in compression. Material ahead of the shock is assumed at rest, and the jump in a quantity is its value in the shocked state minus its value in the initial state. For compression (uniaxial strain) along X_1

$$P = -\sigma_{11}, \quad J = F_{11} = (1 + 2E)^{1/2} = (1 - 2D)^{-1/2}. \quad (2.11)$$

Consider the response of an elastic crystal, without defects. When the internal energy is a linear function of entropy, analytical solutions to the planar shock problem can be derived [Clayton, 2013]. Internal energy functions (to order four in strain) and conjugate thermodynamic stresses for Lagrangian and Eulerian theories, for

uniaxial strain, are

$$\begin{aligned} \bar{U} &= \frac{1}{2}\mathbf{C}_{11}E^2 + \frac{1}{6}\bar{\mathbf{C}}_{111}E^3 \\ &+ \frac{1}{24}\bar{\mathbf{C}}_{1111}E^4 - \theta_0 \left(\Gamma_1 E + \frac{1}{2}\bar{\Gamma}_{11}E^2 - 1 \right) \eta, \quad \bar{S} = -J^{-1}P = \partial\bar{U}/\partial E, \end{aligned} \quad (2.12)$$

$$\begin{aligned} \hat{U} &= \frac{1}{2}\mathbf{C}_{11}D^2 + \frac{1}{6}\hat{\mathbf{C}}_{111}D^3 \\ &+ \frac{1}{24}\hat{\mathbf{C}}_{1111}D^4 - \theta_0 \left(\Gamma_1 D + \frac{1}{2}\hat{\Gamma}_{11}D^2 - 1 \right) \eta, \quad \hat{S} = -J^3P = \partial\hat{U}/\partial D, \end{aligned} \quad (2.13)$$

where $\theta = \theta_0 > 0$ and $U = \eta = 0$ are state data for material ahead of the shock. Second-order elastic constant \mathbf{C}_{11} and first-order Grüneisen parameter Γ_1 are equal for Eulerian and Lagrangian theories. Third-order elastic constants and second-order Grüneisen parameters are related by [Weaver, 1976; Perrin and Delannoy, 1978; Clayton, 2013]

$$\hat{\mathbf{C}}_{111} = \bar{\mathbf{C}}_{111} + 12\mathbf{C}_{11}, \quad \hat{\Gamma}_{11} = \bar{\Gamma}_{11} + 4\Gamma_1. \quad (2.14)$$

Such relationships among elastic constants are addressed in more detail in the Appendix. Simultaneous solution of (2.10)–(2.13) with use of binomial series expansions for $F_{11}(E)$ and $F_{11}(D)$ and leads to the following fifth-order polynomials for entropy η generated across the shock [Clayton, 2013]

$$\eta(E) = \sum_{k=0}^5 a_k E^k, \quad \eta(D) = \sum_{k=0}^5 b_k D^k, \quad (2.15)$$

$$a_0 = b_0 = a_1 = b_1 = a_2 = b_2 = 0, \quad (2.16)$$

$$a_3 = \frac{1}{12\theta_0}(\bar{\mathbf{C}}_{111} + 3\mathbf{C}_{11}) = b_3 = \frac{1}{12\theta_0}(\hat{\mathbf{C}}_{111} - 9\mathbf{C}_{11}), \quad (2.17)$$

$$a_4 = \frac{1}{24}\theta_0^{-1}[\bar{\mathbf{C}}_{1111} + 3\bar{\mathbf{C}}_{111} - 6\mathbf{C}_{11} + \Gamma_1(\bar{\mathbf{C}}_{111} + 3\mathbf{C}_{11})], \quad (2.18)$$

$$b_4 = \frac{1}{24}\theta_0^{-1}[\hat{\mathbf{C}}_{1111} - 9\hat{\mathbf{C}}_{111} - 6\mathbf{C}_{11} + \Gamma_1(\hat{\mathbf{C}}_{111} - 9\mathbf{C}_{11})],$$

$$\begin{aligned} a_5 &= \frac{1}{48}\theta_0^{-1}[2\bar{\mathbf{C}}_{1111} - 6\bar{\mathbf{C}}_{111} + 15\mathbf{C}_{11} \\ &+ \Gamma_1(\bar{\mathbf{C}}_{1111} + 2\bar{\mathbf{C}}_{111} - 9\mathbf{C}_{11}) + \Gamma_1^2(\bar{\mathbf{C}}_{111} + 3\mathbf{C}_{11})], \end{aligned} \quad (2.19)$$

$$\begin{aligned} b_5 &= \frac{1}{48}\theta_0^{-1}[-6\hat{\mathbf{C}}_{1111} - 6\hat{\mathbf{C}}_{111} - 9\mathbf{C}_{11} \\ &+ \Gamma_1(\hat{\mathbf{C}}_{1111} - 6\hat{\mathbf{C}}_{111} - 33\mathbf{C}_{11}) + \Gamma_1^2(\hat{\mathbf{C}}_{111} - 9\mathbf{C}_{11})]. \end{aligned}$$

Lagrangian solution $\eta(E)$ was derived by Thurston [1974]. Eulerian solution $\eta(D)$ has apparently been derived first by the present author [Clayton, 2013]. Conjugate stresses are, to order five in strain measure E or D ,

$$\begin{aligned}\bar{S} = & C_{11}E + \frac{1}{2}\bar{C}_{111}E^2 + \left(\frac{1}{6}\bar{C}_{1111} - \theta_0\Gamma_1a_3\right)E^3 \\ & - \theta_0E^4[(\Gamma_1a_4 + \bar{\Gamma}_{11}a_3) + \theta_0(\Gamma_1a_5 + \bar{\Gamma}_{11}a_4)E],\end{aligned}\quad (2.20)$$

$$\begin{aligned}\hat{S} = & C_{11}D + \frac{1}{2}\hat{C}_{111}D^2 + \left(\frac{1}{6}\hat{C}_{1111} - \theta_0\Gamma_1b_3\right)D^3 \\ & - \theta_0D^4[(\Gamma_1b_4 + \hat{\Gamma}_{11}b_3) + (\Gamma_1b_5 + \hat{\Gamma}_{11}b_4)D].\end{aligned}\quad (2.21)$$

Shock stress P is then obtained from these stresses using (2.11), (2.12)₂, and (2.13)₂ and is fully known as a function of compression ratio $J = V/V_0$. For Lagrangian theory

$$\begin{aligned}P = & -(1 + 2E)^{1/2} \left\{ C_{11}E + \frac{1}{2}\bar{C}_{111}E^2 + \left(\frac{1}{6}\bar{C}_{1111} - \theta_0\Gamma_1a_3\right)E^3 \right. \\ & \left. - \theta_0E^4[(\Gamma_1a_4 + \bar{\Gamma}_{11}a_3) + \theta_0(\Gamma_1a_5 + \bar{\Gamma}_{11}a_4)E] \right\},\end{aligned}\quad (2.22)$$

where E , D and J are related through (2.11)₂. For Eulerian theory

$$\begin{aligned}P = & -(1 - 2D)^{3/2} \left\{ C_{11}D + \frac{1}{2}\hat{C}_{111}D^2 + \left(\frac{1}{6}\hat{C}_{1111} - \theta_0\Gamma_1b_3\right)D^3 \right. \\ & \left. - \theta_0D^4[(\Gamma_1b_4 + \hat{\Gamma}_{11}b_3) + (\Gamma_1b_5 + \hat{\Gamma}_{11}b_4)D] \right\}.\end{aligned}\quad (2.23)$$

Shock velocity D and particle velocity v can then be found using (2.10)₁ and (2.10)₂.

2.3. Application to metallic single crystals

Properties for aluminum (Al), copper (Cu) (both with cubic crystal structure, shocked along cube axis [100]) and magnesium (Mg) (hexagonal crystal structure, shocked normal [a] and parallel [c] to the c -axis [0001]) are listed in Table 1. These cases all represent so-called pure mode directions wherein planar impact with no transmitted shear stress results in a plane wave with a purely longitudinal component, so the one-dimensional analysis of Sec. 2.2 applies exactly. Second- and third-order elastic constants for Al [Thomas, 1968], Cu [Hiki and Granato, 1966], and Mg [Slutsky and Garland, 1957; Naimon, 1971] are isentropic. Third-order constants are converted from mixed coefficients measured ultrasonically. Lagrangian fourth-order constants are obtained from atomic theory for Cu [Wang and Li, 2009]

Table 1. Single crystal properties ($\theta_0 = 295$ K, $C_{\alpha\beta}$ in GPa and ρ_0 in g/cm³).

Property	Al [100]	Cu [100]	Mg [<i>a</i> -axis]	Mg [<i>c</i> -axis]
C_{11}	107	166	59.4	61.6
\bar{C}_{111}	-1080	-1279	-664	-728
\hat{C}_{111}	203	715	49	12
\bar{C}_{1111}	25000	11900	8170	7380
\hat{C}_{1111}	10500	2000	1220	893
Γ_1	2.17	1.97	1.52	1.52
ρ_0	2.70	8.96	1.74	1.74

and Mg [Rao and Padmaja, 1990], and from experimental shock data for Al [Zimmerman *et al.*, 2011]. Grüneisen parameters are obtained from the identity

$$\Gamma_1 = \sum_{\beta=1}^6 C_{1\beta} \alpha_{\beta} / c_P, \quad (2.24)$$

with α_{β} (Voigt notation) and c_P thermal expansion coefficients and specific heat at constant pressure [Wallace, 1972]. Higher-order Grüneisen parameter $\bar{\Gamma}_{11}$ is found assuming $\rho \bar{\Gamma}_{\beta} = \rho_0 \bar{\Gamma}_{0\beta} = \text{constant}$ [Wallace, 1980], leading to $\bar{\Gamma}_{11} = \Gamma_1$ [Clayton, 2013]. Note that for *c*-axis compression of Mg, notation of Table 1 implies $C_{33} \rightarrow C_{11}$ is the longitudinal stiffness normal to the basal plane, and similarly for higher-order constants.

For each crystal, predictions for shock stress versus volume ratio are made using the analytical solutions of Sec. 2.2 for Eulerian and Lagrangian theories, (2.22) and (2.23), respectively. Model predictions of shock stress P normalized by second-order isentropic elastic constant C_{11} are shown in Fig. 1 for Al, Fig. 2 for Cu, Fig. 3 for Mg [*a*-axis] and Fig. 4 for Mg [*c*-axis]. Elastic constants of up to order four are considered in results labeled “4th order”. For Al and Mg, the relationship [Clayton, 2013]

$$\hat{C}_{1111} = \bar{C}_{1111} - 18\bar{C}_{111} - 318C_{11}, \quad (2.25)$$

obtained (see Appendix) by assuming $\partial^4 \bar{U} / \partial F_{11}^4 = \partial^4 \hat{U} / \partial F_{11}^4$ at the initial reference state, was used to determine the Eulerian fourth-order constant. This assumption was unsatisfactory for Cu, so for that material, \hat{C}_{1111} was matched to the Lagrangian 4th order solution. Results labeled “3rd order” and “2nd order” are obtained, respectively, by setting fourth-order and both third- and fourth-order elastic constants to zero.

All longitudinal higher-order elastic constants (i.e., all third- and fourth-order constants) are smaller in magnitude for Eulerian than Lagrangian theory for these metals, as is evident from Table 1. Furthermore, shock stress predictions of 2nd and 3rd order models are generally closer to those of 4th order theory for Eulerian anisotropic elasticity than Lagrangian anisotropic elasticity, as is evident from Figs. 1–4. Table 2 quantifies error (%) of 2nd and 3rd order predictions rela-

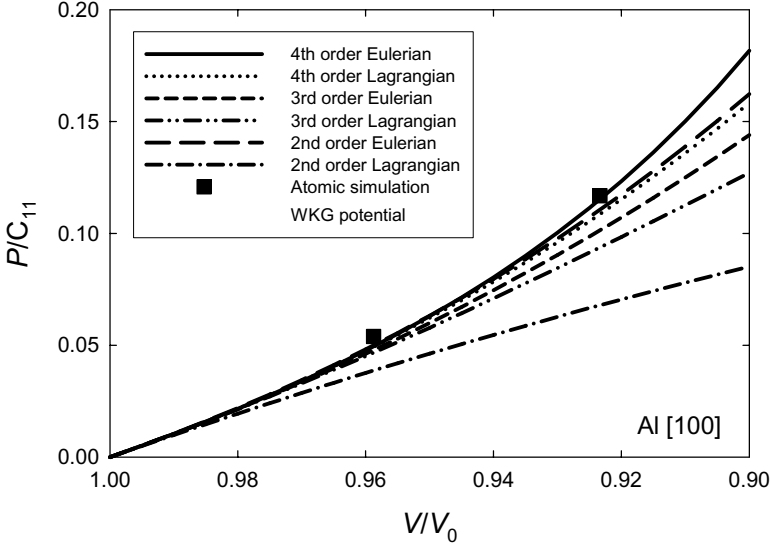


Fig. 1. Axial shock stress in aluminum single crystal shocked elastically along [100] cube axis; atomic simulation data from [Zimmerman *et al.*, 2011].

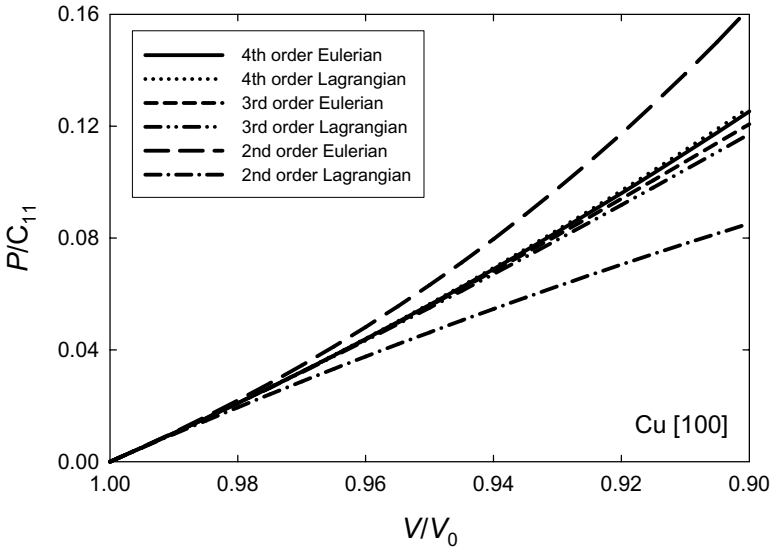


Fig. 2. Axial shock stress in copper single crystal shocked elastically along [100] cube axis.

tive to 4th order predictions, computed as $2 \cdot (2\text{nd or } 3\text{rd order result} - 4\text{th order result}) / (2\text{nd or } 3\text{rd order result} + 4\text{th order result})$. For each crystal type, such errors are almost always smaller in magnitude for Eulerian theory (E2, E3) than for Lagrangian theory (L2, L3) at a given volume ratio and order of approximation.

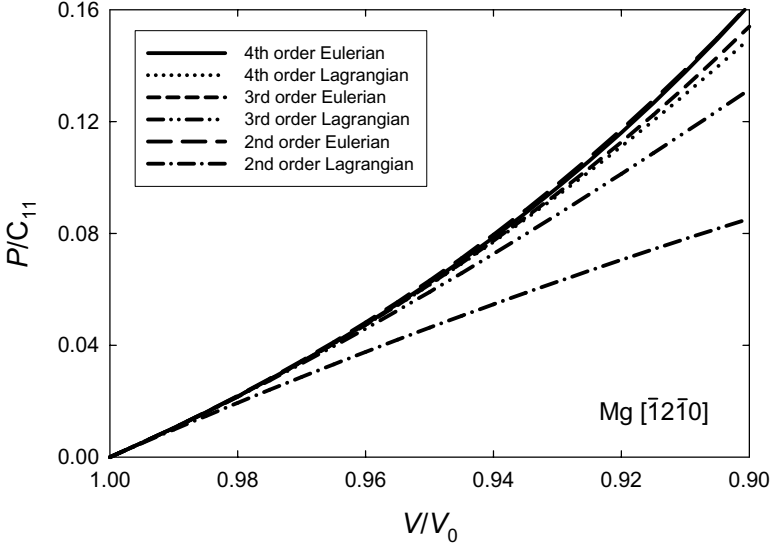


Fig. 3. Axial shock stress in magnesium single crystal shocked elastically along $[\bar{1}2\bar{1}0]$ a -axis.

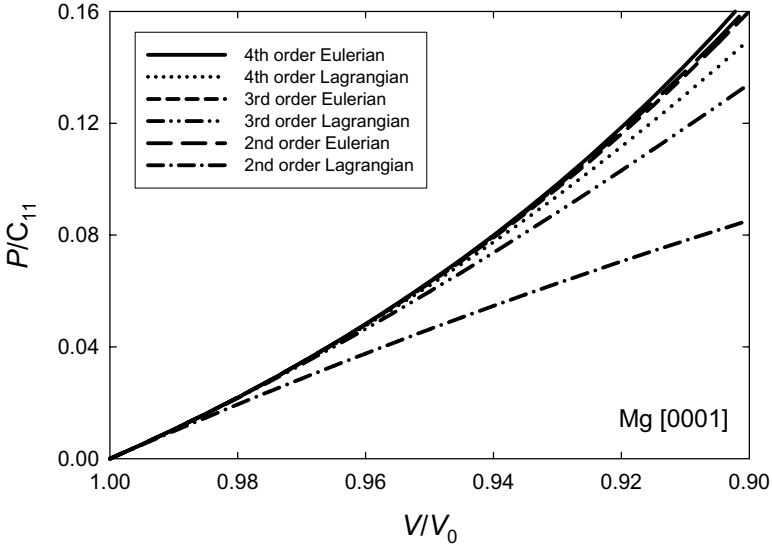


Fig. 4. Axial shock stress in magnesium single crystal shocked elastically along $[0001]$ c -axis.

Together, these observations imply a faster converging series in (2.23) than in (2.22) as the number of higher-order constants is increased, and greater accuracy of Eulerian theory than Lagrangian theory when the same number of elastic constants (i.e., the same order of Taylor polynomial) is used for each internal energy function in

Table 2. Relative error (%) in shock stress P predicted by 2nd (L2, E2) and 3rd (L3, E3) order theories.

V/V_0	Aluminum [100]				Copper [100]				Magnesium [0001]*			
	L3	E3	L2	E2	L3	E3	L2	E2	L3	E3	L2	E2
0.96	-5.0	-3.1	-23.1	+1.1	-1.6	-0.4	-15.8	+9.3	-2.5	-0.4	-23.4	-0.0
0.92	-15.7	-14.1	-48.2	-5.0	-5.4	-2.1	-31.6	+19.9	-7.9	-2.0	-45.1	-1.2
0.88	-28.1	-34.5	-71.2	-19.8	-10.4	-6.2	-46.5	+31.5	-14.5	-5.2	-64.2	-3.8

*Similar trends (i.e., smaller error for Eulerian theory) are obtained for compression along a -axis (not shown).

(2.5)₁. For Al, as shown in Fig. 1, the analytical solution incorporating 4th order Eulerian theory also more closely matches atomic predictions [Zimmerman *et al.*, 2011] of elastic shock stress, with analogous 4th order Lagrangian theory, and all lower order theories, apparently too compliant. At $J = 0.923$, the error in 4th order Lagrangian theory relative to atomic simulation is -7.4% , compared to only -1.4% for 4th order Eulerian theory.

While these results suggest apparent advantages of Eulerian over Lagrangian theory for shock compression of metallic single crystals, it is cautioned that the predictions are purely (thermo)elastic and therefore are strictly applicable only for very small volumes — such as in the aforementioned atomic simulations or in the immediate vicinity of pinned defect cores — wherein plastic deformation does not occur. In laboratory scale specimens, yielding would commence in each of these pure metals at small compressions at which effects of higher-order constants and differences in shock stresses predicted by the two theories would be nearly negligible. However, nonlinear elastic effects on deviatoric stresses could still be important at larger compressions after yielding, particularly for lower symmetry materials with restricted numbers of slip planes/directions [Johnson, 1972], and the nonlinearity in pressure–volume response always becomes important at larger compressions regardless of shear strength, as will be demonstrated explicitly later.

3. Nonlinear Elastic–Plastic Theory

Nonlinear crystal elastoplasticity theory is needed to address the deviatoric response of anisotropic crystals when shear stresses become large enough for defect motion to occur. General continuum frameworks are outlined in Sec. 3.1 wherein elasticity is described by Lagrangian or Eulerian strain measures, and where plasticity is described by shearing on preferred planes in preferred directions. Thermodynamic results are somewhat standard for crystal plasticity with Lagrangian elasticity [Clayton, 2011], but are new for the present kind of Eulerian elasticity. In the context of shock loading, a crystal plasticity framework is also required for proper derivation of driving forces (i.e., conjugate shear stresses) required for slip, twinning, or possible shear fracture in crystals at the onset of yield (i.e., at the HEL) and at higher shock stresses. Analysis of such phenomena is undertaken in Sec. 3.2 via representative

calculations, followed by further consideration of the volumetric response predicted by Lagrangian and Eulerian models.

3.1. Continuum crystal plasticity

Deformation gradient \mathbf{F} of (2.2) is decomposed multiplicatively into elastic and inelastic (i.e., plastic) parts

$$\mathbf{F} = \mathbf{F}^E \mathbf{F}^P, \quad J^E = \det \mathbf{F}^E > 0, \quad J^P = \det \mathbf{F}^P > 0. \quad (3.1)$$

In general, neither \mathbf{F}^E nor \mathbf{F}^P is integrable to a continuous motion field, i.e., these are anholonomic deformations [Clayton, 2012]. The time rate of plastic deformation is dictated by the usual slip kinematics [Asaro, 1983]

$$\dot{\mathbf{F}}^P \mathbf{F}^{P-1} = \sum_{\alpha} \dot{\gamma}^{\alpha} \mathbf{s}_0^{\alpha} \otimes \mathbf{m}_0^{\alpha}, \quad (3.2)$$

with $\dot{\gamma}^{\alpha}$, \mathbf{s}_0^{α} and \mathbf{m}_0^{α} the shearing rate, initial slip direction and initial slip plane normal for glide system α . The latter two vectors deform with the lattice according to

$$\mathbf{s}^{\alpha} = \mathbf{F}^E \mathbf{s}_0^{\alpha}, \quad \mathbf{m}^{\alpha} = \mathbf{F}^{E-T} \mathbf{m}_0^{\alpha}, \quad (3.3)$$

and since $\mathbf{s}_0^{\alpha} \cdot \mathbf{m}_0^{\alpha} = \mathbf{s}^{\alpha} \cdot \mathbf{m}^{\alpha} = 0$, plastic deformation is isochoric

$$\dot{J}^P = J^P \text{tr}(\dot{\mathbf{F}}^P \mathbf{F}^{P-1}) = 0, \quad J^P = 1, \quad J = J^E. \quad (3.4)$$

Ignored are possible contributions to residual deformation and plastic volume change from nonlinear elastic and core effects that may be non-negligible when defect densities become very large [Teodosiu, 1982; Clayton *et al.*, 2014]. Such effects could be incorporated explicitly via insertion of a third term in decomposition (3.1) [Clayton *et al.*, 2005; Clayton *et al.*, 2014], but are not considered further in this work, which relies on the traditional two-term kinematic decomposition of crystal plasticity [Asaro, 1983]. Lagrangian and Eulerian strain tensors of (2.3) are redefined here as their purely elastic counterparts

$$\mathbf{E} = \frac{1}{2}(\mathbf{F}^{ET} \mathbf{F}^E - \mathbf{1}), \quad \mathbf{D} = \frac{1}{2}(\mathbf{1} - \mathbf{F}^{E-1} \mathbf{F}^{E-T}). \quad (3.5)$$

The usual continuum balance laws in (2.4) still apply, again for the adiabatic case. Respective thermodynamic potentials for Lagrangian and Eulerian theories are now

$$U = \bar{U}(\mathbf{E}, \eta, \zeta), \quad U = \hat{U}(\mathbf{D}, \eta, \zeta); \quad \Psi = \bar{\Psi}(\mathbf{E}, \theta, \zeta), \quad \Psi = \hat{\Psi}(\mathbf{D}, \theta, \zeta). \quad (3.6)$$

Scalar internal state variable ζ accounts for energy of lattice defects, e.g., stored energy of cold work associated with microscopic stress fields of dislocations and their core energies [Rosakis *et al.*, 2000; Clayton *et al.*, 2014]. Replacement of ζ with a vector or higher-order tensor state variable(s) poses no conceptual difficulties, as has been demonstrated elsewhere for Lagrangian crystal elastoplasticity [Luscher *et al.*, 2013].

For Lagrangian elasticity theory, thermoelastic constitutive relations for stress (3.7)₁, temperature (3.7)₂; entropy (3.7)₃; conjugate force to defect density (3.7)₄; the temperature rate form of the local energy balance (3.8)₁; the reduced entropy inequality (3.8)₂; and the conjugate driving force (resolved Kirchhoff stress [Asaro, 1983]) for slip (3.9) are derived from (2.4) and (3.1)–(3.6) using standard principles [Rosakis *et al.*, 2000; Clayton, 2011; Luscher *et al.*, 2013]

$$\bar{\mathbf{S}} = \frac{\partial \bar{U}}{\partial \mathbf{E}} = \frac{\partial \bar{\Psi}}{\partial \mathbf{E}} = J \mathbf{F}^{E-1} \boldsymbol{\sigma} \mathbf{F}^{E-T}, \quad \theta = \partial \bar{U} / \partial \eta, \quad \eta = -\partial \bar{\Psi} / \partial \theta, \quad \bar{\chi} = -\partial \bar{\Psi} / \partial \zeta, \quad (3.7)$$

$$\bar{c}\dot{\theta} = \sum_{\alpha} \bar{\tau}^{\alpha} \dot{\gamma}^{\alpha} + \theta \frac{\partial \bar{\mathbf{S}}}{\partial \theta} : \dot{\mathbf{E}} + \left(\bar{\chi} - \theta \frac{\partial \bar{\chi}}{\partial \theta} \right) \dot{\zeta}; \quad \sum_{\alpha} \bar{\tau}^{\alpha} \dot{\gamma}^{\alpha} + \bar{\chi} \dot{\zeta} \geq 0, \quad (3.8)$$

$$\bar{\tau}^{\alpha} = J \boldsymbol{\sigma} : \mathbf{s}^{\alpha} \otimes \mathbf{m}^{\alpha} = (\mathbf{F}^{ET} \mathbf{F}^E \bar{\mathbf{S}}) : \mathbf{s}_0^{\alpha} \otimes \mathbf{m}_0^{\alpha}. \quad (3.9)$$

For Eulerian elasticity theory, the analogous thermodynamic relationships are derived as

$$\hat{\mathbf{S}} = \frac{\partial \hat{U}}{\partial \mathbf{D}} = \frac{\partial \hat{\Psi}}{\partial \mathbf{D}} = J \mathbf{F}^{ET} \boldsymbol{\sigma} \mathbf{F}^E, \quad \theta = \partial \hat{U} / \partial \eta, \quad \eta = -\partial \hat{\Psi} / \partial \theta, \quad \hat{\chi} = -\partial \hat{\Psi} / \partial \zeta, \quad (3.10)$$

$$\hat{c}\dot{\theta} = \sum_{\alpha} \hat{\tau}^{\alpha} \dot{\gamma}^{\alpha} + \theta \frac{\partial \hat{\mathbf{S}}}{\partial \theta} : \dot{\mathbf{D}} + \left(\hat{\chi} - \theta \frac{\partial \hat{\chi}}{\partial \theta} \right) \dot{\zeta}; \quad \sum_{\alpha} \hat{\tau}^{\alpha} \dot{\gamma}^{\alpha} + \hat{\chi} \dot{\zeta} \geq 0, \quad (3.11)$$

$$\hat{\tau}^{\alpha} = J \boldsymbol{\sigma} : \mathbf{s}^{\alpha} \otimes \mathbf{m}^{\alpha} = (\hat{\mathbf{S}} \mathbf{F}^{E-1} \mathbf{F}^{E-T}) : \mathbf{s}_0^{\alpha} \otimes \mathbf{m}_0^{\alpha}. \quad (3.12)$$

On the right-hand sides of energy balances (3.8)₁, and (3.11)₁, the first terms represent plastic dissipation, the second terms represent thermoelastic coupling due to thermal expansion/contraction, and the rightmost terms represent stored energy accumulation with defects generated during deformation, for example. As defined in (3.7)₄ and (3.10)₄, χ is the conjugate thermodynamic force to internal state variable ζ [Rice, 1971]. The product of χ and the time rate of ζ gives the free energy dissipation rate (if positive) or free energy storage rate (if negative) associated with evolution of the local defect arrangement (such as dislocation density) and corresponding residual stress state.

Governing equations for the two elasticity representations are remarkably similar, the only crucial differences being the different stress tensors in hyperelastic laws of (3.7)₁ and (3.10)₁ and resulting differences in thermodynamic driving forces for slip in (3.9) and (3.12). It is remarked that quantitative differences in resolved shear stresses (3.9) and (3.12) arise solely from truncation of Taylor polynomials corresponding to (3.6) at a given order in strain measure \mathbf{E} or \mathbf{D} . For elastic strains that are not too large (e.g., magnitude less than unity), such Taylor polynomials should converge to give the same values of resolved shear stress if a sufficient number of

terms (i.e., a sufficient number of higher-order elastic constants) is included in each polynomial. Physically, the definition of each of (3.9) and (3.12) is identical: The shear stress (current force per unit reference area or energy per unit reference volume [Asaro, 1983]) acting in the direction of slip (or parallel to the Burgers vector) and resolved on the plane of dislocation glide.

General theories are complete upon prescription of kinetic equations for inelastic deformation and defects, e.g., for Lagrangian theory

$$\dot{\gamma}^\alpha = \dot{\gamma}^\alpha(\bar{\tau}^\alpha; \theta, \zeta), \quad \dot{\zeta} = \dot{\zeta}(\bar{\chi}; \mathbf{E}, \theta). \quad (3.13)$$

For Eulerian elasticity,

$$\dot{\gamma}^\alpha = \dot{\gamma}^\alpha(\hat{\tau}^\alpha; \theta, \zeta), \quad \dot{\zeta} = \dot{\zeta}(\hat{\chi}; \mathbf{D}, \theta). \quad (3.14)$$

The first of (3.13) and (3.14) apply for viscoplastic slip. For idealized rate independent plasticity with slip resistance (shear strength) g^α depending possibly on temperature and defect content, these slip rate equations could be replaced with [Asaro, 1983]

$$\bar{\tau}^\alpha < g^\alpha(\theta, \zeta) \Leftrightarrow \dot{\gamma}^\alpha = 0, \quad \bar{\tau}^\alpha = g^\alpha(\theta, \zeta) \Leftrightarrow |\dot{\gamma}^\alpha| \geq 0, \quad (3.15)$$

$$\hat{\tau}^\alpha < g^\alpha(\theta, \zeta) \Leftrightarrow \dot{\gamma}^\alpha = 0, \quad \hat{\tau}^\alpha = g^\alpha(\theta, \zeta) \Leftrightarrow |\dot{\gamma}^\alpha| \geq 0. \quad (3.16)$$

Expanding internal energy functions as Taylor polynomials of order three in respective elastic strain measures, order two in entropy and ζ , and bilinear in the product of strain and entropy, (3.6) produces

$$\bar{U} = \frac{1}{2}C_{\alpha\beta}E_\alpha E_\beta + \frac{1}{6}\bar{C}_{\alpha\beta\chi}E_\alpha E_\beta E_\chi + \theta_0\eta \left[1 - \Gamma_\alpha E_\alpha + \frac{1}{2c}\eta \right] + \frac{1}{2}\mu\zeta^2, \quad (3.17)$$

$$\hat{U} = \frac{1}{2}C_{\alpha\beta}D_\alpha D_\beta + \frac{1}{6}\hat{C}_{\alpha\beta\chi}D_\alpha D_\beta D_\chi + \theta_0\eta \left[1 - \Gamma_\alpha D_\alpha + \frac{1}{2c}\eta \right] + \frac{1}{2}\mu\zeta^2, \quad (3.18)$$

where summation applies over Greek indices denoting Voigt notation ($\alpha = 1, 2, \dots, 6$). Second- and third-order isentropic elastic constants are

$$C_{\alpha\beta} = \left. \frac{\partial^2 \bar{U}}{\partial E_\alpha \partial E_\beta} \right|_0 = \left. \frac{\partial^2 \hat{U}}{\partial D_\alpha \partial D_\beta} \right|_0, \quad \bar{C}_{\alpha\beta\chi} = \left. \frac{\partial^3 \bar{U}}{\partial E_\alpha \partial E_\beta \partial E_\chi} \right|_0, \quad (3.19)$$

$$\hat{C}_{\alpha\beta\chi} = \left. \frac{\partial^3 \hat{U}}{\partial D_\alpha \partial D_\beta \partial D_\chi} \right|_0,$$

with a zero subscript denoting evaluation at the unstressed reference state at ambient temperature θ_0 . Relationships between third-order Lagrangian and Eulerian constants in (3.19)₂ and (3.19)₃ are analogous to those of the purely elastic theory derived in (A.8) of the Appendix. Ambient specific heat at fixed strain and Grüneisen parameters are equivalent in Lagrangian and Eulerian representations

$$c = \partial \bar{U} / \partial \theta|_0 = \partial \hat{U} / \partial \theta|_0, \quad \theta_0 \Gamma_\alpha = -\partial^2 \bar{U} / \partial E_\alpha \partial \eta|_0 = -\partial^2 \hat{U} / \partial D_\alpha \partial \eta|_0. \quad (3.20)$$

Residual energy of lattice defects is represented by the rightmost terms in (3.17) and (3.18). When ζ is dimensionless, μ can be taken proportional to a representative

shear modulus G_0 . For example, letting φ denote the total dislocation line length per unit volume, b the magnitude of a typical Burgers vector, and k a dimensionless parameter of typical order unity, a physically realistic assumption is [Clayton, 2011]

$$\zeta = b\sqrt{\phi}, \quad \frac{1}{2}\mu\zeta^2 = \frac{1}{2}\kappa G_0 b^2 \phi. \quad (3.21)$$

3.2. *Nonlinear elastic effects on yielding and pressure in shock compression*

For crystals of symmetric orientations^b subjected to planar shock loading above the HEL, a two-wave structure appears consisting of an elastic precursor followed by a slower-moving plastic wave (presuming the shock is not overdriven), both waves characterized by purely longitudinal particle motion. The shock stress at the HEL, according to the model of Sec. 3.1 and written as P_H , is attained when slip rates in (3.13)–(3.16) first become nonzero. In rate independent theory, this corresponds to resolved shear stresses of (3.9) or (3.12) attaining critical values g^α . Assuming such critical strength values are known, the model of Sec. 3.1 can be used to analytically determine P_H , and the corresponding volume ratio at the HEL, V_H/V_0 , or vice-versa, assuming no plastic deformation or defect generation takes place for (thermo)elastic loading up to the HEL. Similar nonlinear elastic analyses have been used to infer material strength from experimental longitudinal shock data [Lang and Gupta, 2010; Turneare and Gupta, 2011]. The importance of using nonlinear elastic rather than linear elastic models for such calculations has been demonstrated elsewhere [Turneare and Gupta, 2011]. In what follows next, differences in strength predictions resulting from different choices of nonlinear elastic model (i.e., Lagrangian versus Eulerian) are computed for several representative cases.

In order to restrict the number of parameters entering the analysis, an ideal solid with isotropic symmetry in second-order elastic constants and simultaneous isotropic and Cauchy symmetry in third-order elastic constants is now considered [Clayton, 2013]. Cauchy symmetry of third-order constants is representative of several noble metals [Hiki *et al.*, 1966]. Isentropic second-order elastic constants are, in terms of bulk modulus B_0 and Poisson's ratio ν

$$C_{11} = 3\frac{1-\nu}{1+\nu}B_0, \quad C_{12} = 3\frac{\nu}{1+\nu}B_0, \quad C_{44} = G_0 = \frac{3}{2}\frac{1-2\nu}{1+\nu}B_0. \quad (3.22)$$

Isentropic third-order constants are, in terms of B_0 and its pressure derivative B'_0

$$\bar{C}_{111} = 5\bar{C}_{112} = 15\bar{C}_{123} = -\frac{27}{7}B'_0B_0, \quad \hat{C}_{111} = 5\hat{C}_{112} = 15\hat{C}_{123} = -\frac{27}{7}(B'_0 - 4)B_0. \quad (3.23)$$

^bFor orientations of lower symmetry, the response to step loading in normal stress generally consists of quasi-longitudinal elastic and plastic waves and multiple quasi-transverse elastic and plastic waves [Johnson, 1972].

Uniaxial strain conditions for plane wave propagation in the X_1 -direction are again considered, where up to the HEL, with φ_0 denoting the initial dislocation density

$$\mathbf{F}^P = \mathbf{1}, \quad J = F_{11}^E = F_{11} = V/V_0, \quad \varphi = \varphi_0 = \text{constant}. \quad (3.24)$$

Equations (2.15)–(2.23) still apply, but many reduce to simpler forms. Internal energy functions (3.17) and (3.18) become

$$\bar{U} = \left(\frac{3}{2} \frac{1-\nu}{1+\nu} - \frac{9}{14} \mathbf{B}'_0 E \right) \mathbf{B}_0 E^2 - \theta_0 (\Gamma E - 1) \eta + \frac{3}{4} \frac{1-2\nu}{1+\nu} \kappa b^2 \mathbf{B}_0 \varphi_0, \quad (3.25)$$

$$\hat{U} = \left[\frac{3}{2} \frac{1-\nu}{1+\nu} - \frac{9}{14} (\mathbf{B}'_0 - 4) D \right] \mathbf{B}_0 D^2 - \theta_0 (\Gamma D - 1) \eta + \frac{3}{4} \frac{1-2\nu}{1+\nu} \kappa b^2 \mathbf{B}_0 \varphi_0, \quad (3.26)$$

where the quadratic term in entropy is omitted for purely elastic shocks [Thurston, 1974].

To order three in strains, longitudinal thermodynamic stress components are

$$\bar{S}_{11} = \left(3 \frac{1-\nu}{1+\nu} - \frac{27}{14} \mathbf{B}'_0 E \right) \mathbf{B}_0 E + \left(\frac{9}{28} \mathbf{B}'_0 - \frac{3}{4} \frac{1-\nu}{1+\nu} \right) \Gamma \mathbf{B}_0 E^3, \quad (3.27)$$

$$\hat{S}_{11} = \left[3 \frac{1-\nu}{1+\nu} - \frac{27}{14} (\mathbf{B}'_0 - 4) D \right] \mathbf{B}_0 D + \left[\frac{9}{28} (\mathbf{B}'_0 - 4) + \frac{9}{4} \frac{1-\nu}{1+\nu} \right] \Gamma \mathbf{B}_0 D^3. \quad (3.28)$$

Terms cubic in either strain measure result from entropy production across the shock. Nonzero Cauchy stress components are then, for Lagrangian theory

$$\begin{aligned} \sigma_{11} = -P &= (1 + 2E)^{1/2} \left[\left(3 \frac{1-\nu}{1+\nu} - \frac{27}{14} \mathbf{B}'_0 E \right) \mathbf{B}_0 E \right. \\ &\quad \left. + \left(\frac{9}{28} \mathbf{B}'_0 - \frac{3}{4} \frac{1-\nu}{1+\nu} \right) \Gamma \mathbf{B}_0 E^3 \right], \end{aligned} \quad (3.29)$$

$$\begin{aligned} \sigma_{22} = \sigma_{33} &= (1 + 2E)^{-1/2} \left[\left(3 \frac{\nu}{1+\nu} - \frac{27}{70} \mathbf{B}'_0 E \right) \mathbf{B}_0 E \right. \\ &\quad \left. + \left(\frac{9}{28} \mathbf{B}'_0 - \frac{3}{4} \frac{1-\nu}{1+\nu} \right) \Gamma \mathbf{B}_0 E^3 \right]. \end{aligned} \quad (3.30)$$

Analogously, for Eulerian theory,

$$\begin{aligned} \sigma_{11} = -P &= (1 - 2D)^{3/2} \left\{ \left[3 \frac{1-\nu}{1+\nu} - \frac{27}{14} (\mathbf{B}'_0 - 4) D \right] \mathbf{B}_0 D \right. \\ &\quad \left. + \left[\frac{9}{28} (\mathbf{B}'_0 - 4) + \frac{9}{4} \frac{1-\nu}{1+\nu} \right] \Gamma \mathbf{B}_0 D^3 \right\}, \end{aligned} \quad (3.31)$$

$$\begin{aligned} \sigma_{22} = \sigma_{33} &= (1 - 2D)^{1/2} \left\{ \left[3 \frac{\nu}{1+\nu} - \frac{27}{70} (\mathbf{B}'_0 - 4) D \right] \mathbf{B}_0 D \right. \\ &\quad \left. + \left[\frac{9}{28} (\mathbf{B}'_0 - 4) + \frac{9}{4} \frac{1-\nu}{1+\nu} \right] \Gamma \mathbf{B}_0 D^3 \right\}. \end{aligned} \quad (3.32)$$

Resolved shear stresses from (3.9) and (3.12) are, respectively

$$\begin{aligned}
 \bar{\tau}^\alpha &= (1 + 2E) \left[\left(3 \frac{1 - \nu}{1 + \nu} - \frac{27}{14} B'_0 E \right) B_0 E \right. \\
 &\quad \left. + \left(\frac{9}{28} B'_0 - \frac{3}{4} \frac{1 - \nu}{1 + \nu} \right) \Gamma B_0 E^3 \right] s_1^\alpha m_1^\alpha \\
 &\quad + \left[\left(3 \frac{\nu}{1 + \nu} - \frac{27}{70} B'_0 E \right) B_0 E \right. \\
 &\quad \left. + \left(\frac{9}{28} B'_0 - \frac{3}{4} \frac{1 - \nu}{1 + \nu} \right) \Gamma B_0 E^3 \right] (s_2^\alpha m_2^\alpha + s_3^\alpha m_3^\alpha), \tag{3.33}
 \end{aligned}$$

$$\begin{aligned}
 \hat{\tau}^\alpha &= (1 - 2D) \left\{ \left[3 \frac{1 - \nu}{1 + \nu} - \frac{27}{14} (B'_0 - 4) D \right] B_0 D \right. \\
 &\quad \left. + \left[\frac{9}{28} (B'_0 - 4) + \frac{9}{4} \frac{1 - \nu}{1 + \nu} \right] \Gamma B_0 D^3 \right\} s_1^\alpha m_1^\alpha \\
 &\quad + \left\{ \left[3 \frac{\nu}{1 + \nu} - \frac{27}{70} (B'_0 - 4) D \right] B_0 D \right. \\
 &\quad \left. + \left[\frac{9}{28} (B'_0 - 4) + \frac{9}{4} \frac{1 - \nu}{1 + \nu} \right] \Gamma B_0 D^3 \right\} (s_2^\alpha m_2^\alpha + s_3^\alpha m_3^\alpha), \tag{3.34}
 \end{aligned}$$

noting that under the present uniaxial strain loading conditions

$$\mathbf{J}\boldsymbol{\sigma} : \mathbf{s}^\alpha \otimes \mathbf{m}^\alpha = \mathbf{J}\boldsymbol{\sigma} : \mathbf{s}_0^\alpha \otimes \mathbf{m}_0^\alpha = J(\sigma_{11} s_1^\alpha m_1^\alpha + \sigma_{22} s_2^\alpha m_2^\alpha + \sigma_{33} s_3^\alpha m_3^\alpha). \tag{3.35}$$

Temperatures in respective Lagrangian and Eulerian solutions are simply

$$\theta = \partial \bar{U} / \partial \eta = \theta_0 (1 - \Gamma E), \quad \theta = \partial \hat{U} / \partial \eta = \theta_0 (1 - \Gamma D). \tag{3.36}$$

Two representative slip configurations are considered: (i) Octahedral slip in a cubic crystal shocked along the cube axis [100] and (ii) prismatic slip in a hexagonal crystal shocked along the a -axis [$\bar{1}2\bar{1}0$]. Both of these configurations represent pure mode directions, whereby symmetry would lead to purely longitudinal elastic and plastic waves. For initiation of octahedral slip, eight of the twelve $\{111\}\langle\bar{1}\bar{1}0\rangle$ type systems in a face-centered-cubic (FCC) crystal would be subjected to an equal resolved shear stress τ^α , the remaining four unstressed [Johnson *et al.*, 1970]. The same solution would apply for $\{110\}\langle\bar{1}\bar{1}1\rangle$ slip in a body-centered-cubic (BCC) crystal, with \mathbf{s}^α and \mathbf{m}^α simply interchanged in (3.33)–(3.35). Representative slip vectors are taken as

$$\mathbf{s}_0 = (1/\sqrt{2}, -1/\sqrt{2}, 0), \quad \mathbf{m}_0 = (1/\sqrt{3}, 1/\sqrt{3}, 1/\sqrt{3}). \tag{3.37}$$

For initiation of prismatic slip, two of the three $\{10\bar{1}0\}\langle\bar{1}2\bar{1}0\rangle$ systems would be subjected to an equal resolved shear stress, the third unstressed [Johnson, 1974], and

$$\mathbf{s}_0 = (-1/2, \sqrt{3}/2, 0), \quad \mathbf{m}_0 = (\sqrt{3}/2, 1/2, 0). \tag{3.38}$$

Resolved shear stress magnitudes obtained from Lagrangian theory by (3.33) and Eulerian theory by (3.34) are shown in Fig. 5 for octahedral slip system (3.37) and in Fig. 6 for prismatic system (3.38). In each case, the pressure derivative of the bulk modulus and the Grüneisen parameter are fixed at representative values

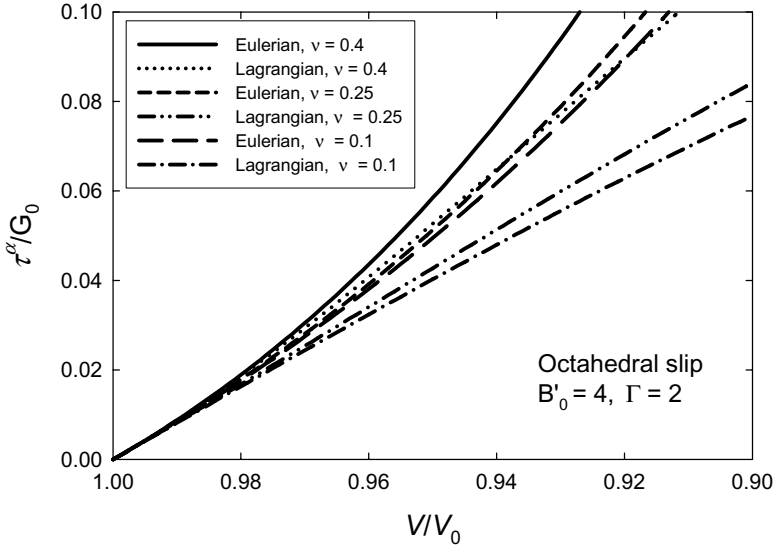


Fig. 5. Resolved shear stress on $\{111\}\langle 1\bar{1}0 \rangle$ systems for shock loading along $[100]$.

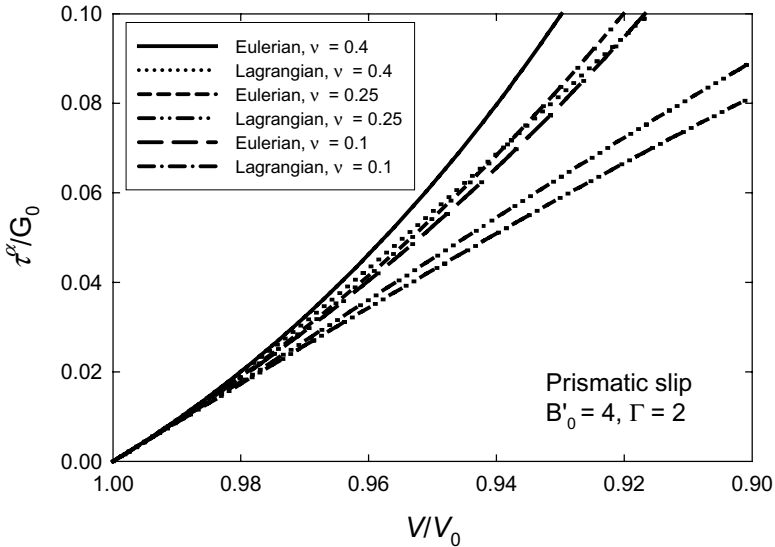


Fig. 6. Resolved shear stress on $\{10\bar{1}0\}\langle \bar{1}2\bar{1}0 \rangle$ systems for shock loading along $[\bar{1}2\bar{1}0]$.

of 4 and 2, respectively, and Poisson's ratio is varied from 0.1 to 0.4. Shear stresses are normalized by the elastic shear modulus. Differences in predictions of Eulerian and Lagrangian theories emerge at volumetric compression ratio (V/V_0) less than 0.99, i.e., at greater than about 1% uniaxial compression. For a fixed value of Poisson's ratio ν , shear stresses predicted by Eulerian elasticity tend to exceed those predicted by Lagrangian elasticity. Normalized shear stresses tend to increase with increasing ν because shear modulus G_0 decreases rapidly relative to the bulk modulus as Poisson's ratio increases.

Table 3 shows resolved shear stresses predicted by each theory at the same value of HEL stress P_H . These are the slip strengths that would be extracted from plate impact data on P_H . For HEL stresses on the order of 1% of the ambient bulk modulus or less, differences between Lagrangian and Eulerian predictions are negligible, as inferred from the first row of Table 3. This would be the case for very ductile metals, for example. However, differences between Lagrangian and Eulerian theories become significant for strong solids with larger elastic limits. The case $P_H/B_0 = 0.1$ is physically representative of prismatic slip in shock-compressed sapphire [Graham and Brooks, 1971; Clayton, 2009] or silicon carbide [Clayton, 2010]. The case $P_H/B_0 = 0.25$ is physically representative of octahedral slip in diamond [Lang and Gupta, 2010]. In the latter case, the difference in predictions of the two elasticity models is on the order of 20%. Slip resistance also often depends on temperature. Temperature rise predicted by Lagrangian and Eulerian theories through (3.36) is compared in Fig. 7. Discernible differences emerge at compressions exceeding 3%. Cleavage fracture is known to occur on preferred planes in crystals, and perhaps in preferential directions due to lattice trapping [Riedle *et al.*, 1996]. Results of foregoing analysis may apply to such fractures.

For solids with relatively low shear strength (e.g., $g^\alpha \leq 0.01B_0$), shock stress P above the HEL does not greatly exceed Cauchy pressure p , and deviatoric stresses become negligible with respect to pressure. This is the case for many pure ductile polycrystalline metals, and is approximately true for ductile single crystals when stresses are sufficient to enable slip on primary and secondary systems so that the response is reasonably isotropic [Johnson, 1974]. The same statements would apply to brittle solids with low fracture strengths on a sufficient number of planes. A standard assumption for isotropic solids under such conditions is that the shock

Table 3. Resolved shear stresses at HEL stress P_H with $\nu = 0.25$, $B'_0 = 4$ and $\Gamma = 2$.

P_H/B_0	$\bar{\tau}^\alpha/G_0$ octahedral	$\hat{\tau}^\alpha/G_0$ octahedral	$\bar{\tau}^\alpha/G_0$ prismatic	$\hat{\tau}^\alpha/G_0$ prismatic
0.010	0.0045	0.0045	0.0048	0.0048
0.025	0.0112	0.0114	0.0118	0.0120
0.050	0.0219	0.0227	0.0233	0.0241
0.100	0.0423	0.0451	0.0449	0.0478
0.250	0.0939	0.1107	0.0996	0.1174

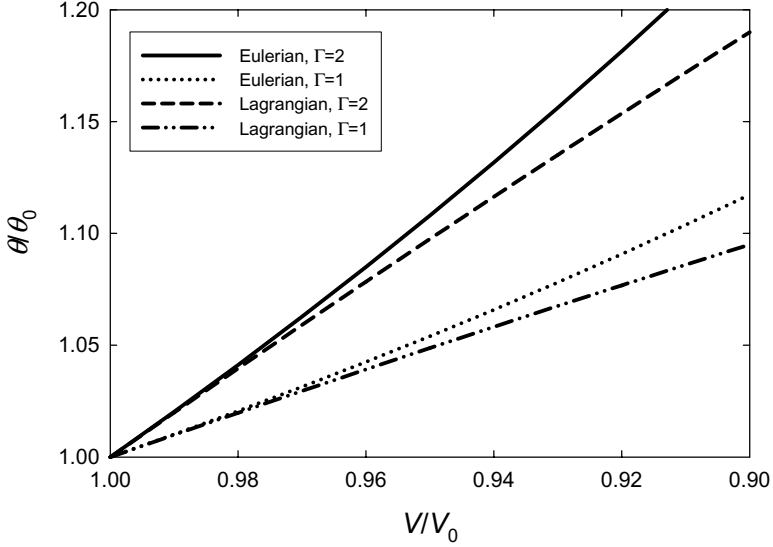


Fig. 7. Temperature rise versus volume ratio for elastic shock loading.

pressure can be adequately represented by a scalar EOS, i.e., $P \approx p$ [Germain and Lee, 1973; Jeanloz, 1989]. If isentropic conditions are assumed, as in (2.8) and (2.9), then differences between shock pressure P and isentropic hydrostat p are due to shear strength and entropy production (e.g., from thermoelasticity and viscous

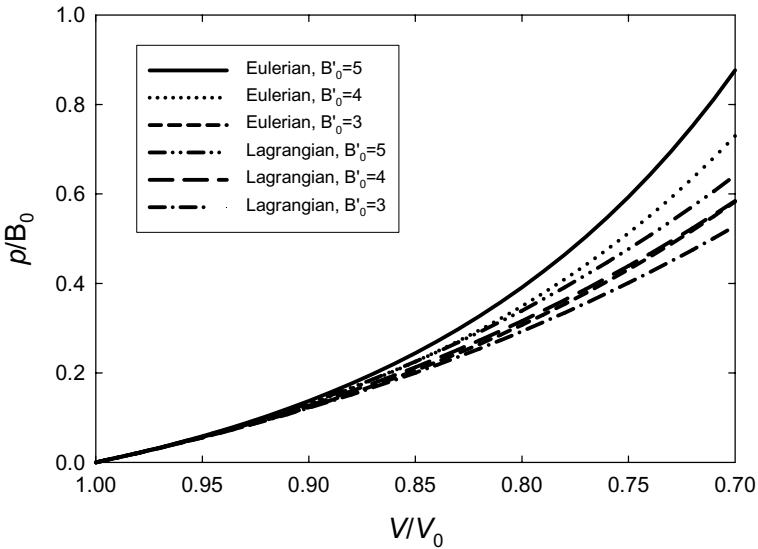


Fig. 8. Pressure under hydrostatic compression, generic isotropic solid.

dissipation) that would occur during the shock process. Predictions of third-order Lagrangian EOS (2.8) and third-order Eulerian EOS (2.9) are compared in Fig. 8 over a physically realistic range of B'_0 . Differences between the two become apparent at compressions exceeding about 5%, with Eulerian theory producing relatively higher pressure than Lagrangian theory for a material compressed to the same specific volume.

Polycrystalline aluminum and copper have dynamic deviatoric strengths $g^\alpha < 0.01B_0$. Comparison of shock data with hydrostatic compression data [Mao *et al.*, 1978; Greene *et al.*, 1994] demonstrates that a scalar EOS should suffice for describing the response of these metals shocked compressed over $0.95 > V/V_0 > 0.75$. Magnesium exhibits relatively low resistance to slip and/or twinning in various directions [Clayton and Knap, 2011, 2013; Wu *et al.*, 2012] and thus a scalar EOS should also be appropriate for untextured Mg polycrystals at moderate compressions. Predictions of each third-order EOS in (2.8) and (2.9) are compared with experimental shock compression data [Marsh *et al.*, 1980] for Al in Fig. 9, Cu in Fig. 10, and Mg in Fig. 11. Compressibility properties of Table 4 used in these predictions are obtained from ultrasonic experiments at small compression [Guinan and Steinberg, 1974] and are not fit to the shock compression data. In each case, superior agreement of Eulerian theory with the data is apparent. Jeanloz [1989] suggested that an Eulerian EOS should be more accurate than a Lagrangian EOS of the same order for most pure substances, in agreement with the particular metals analyzed here.

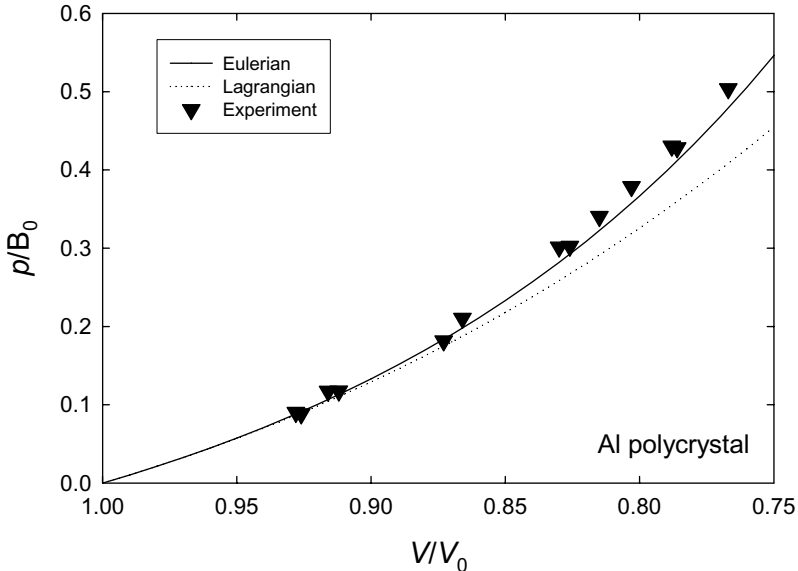


Fig. 9. Predictions of Eulerian and Lagrangian EOS and shock compression data for aluminum [Marsh, 1980].

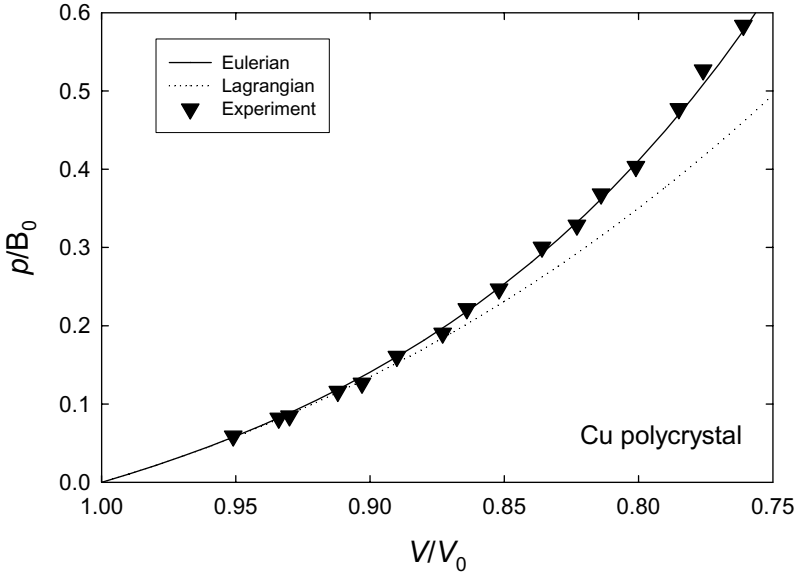


Fig. 10. Predictions of Eulerian and Lagrangian EOS and shock compression data for copper [Marsh, 1980].

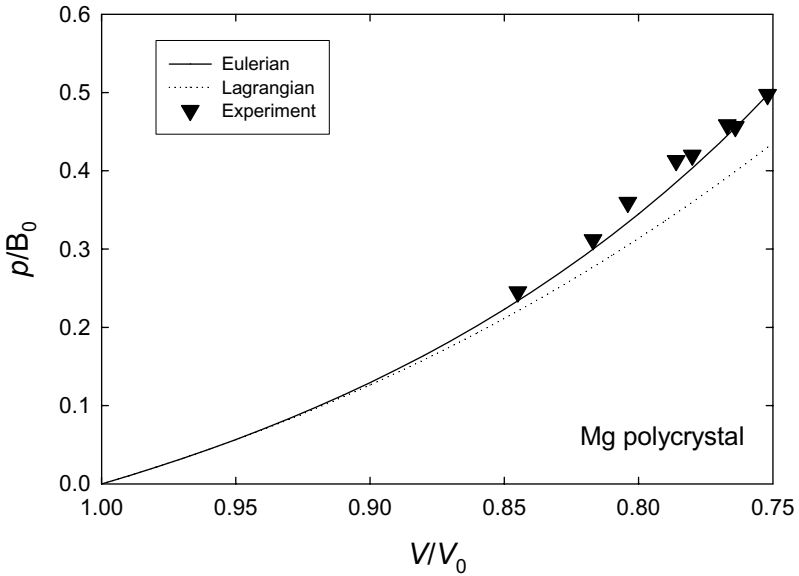


Fig. 11. Predictions of Eulerian and Lagrangian EOS and shock data for magnesium [Marsh, 1980].

Table 4. Isentropic bulk modulus (GPa) and its pressure derivative [Guinan and Steinberg, 1974].

Material	B_0	B'_0
Al	76	4.42
Cu	137	5.48
Mg	35.4	3.90

4. Discussion

Results and analysis in Secs. 2.3 and 3.2 suggest that overall, Eulerian theory should provide a more accurate depiction than Lagrangian theory of the mechanical response of metallic crystals under spherical compression and uniaxial strain compression, in particular when internal energy functions are truncated at orders two or three in corresponding finite strain measures. This assertion can be understood to follow from the physical observation that in typical metallic crystals, strain energy density, stress or pressure, longitudinal stiffness, and tangent bulk modulus all tend to increase rapidly with decreasing specific volume, and from the mathematical observation that components of Eulerian strain increase more rapidly in magnitude in compression (become more largely negative) than do components of Lagrangian strain, as demonstrated explicitly in Table 5. For example, second-order Eulerian elasticity tends to predict significantly larger (in magnitude) axial stress than second-order Lagrangian theory since in second-order theories, thermodynamic stresses are linearly related to work conjugate strains. It is clarified that the results and analysis herein do not necessarily favor one strain measure over the other for general descriptions of continuum kinematics. Rather, they support the notion that a finite Taylor series representation of internal energy in Eulerian tensor \mathbf{D} appears advantageous to one of the same order in Lagrangian tensor \mathbf{E} for describing the stress response of possibly anisotropic metallic materials under finite compressive strain. Furthermore, although such Taylor series representations of energy are mathematically rigorous and convenient for general anisotropic solids since they incorporate correct symmetries through corresponding independent elastic constants, such polynomial forms may not necessarily be ideal for describing particular materials. Another drawback for such higher-order theories is that elastic constants of order

Table 5. Axial strain components under spherical and uniaxial deformation.

V/V_0	Spherical strain		Uniaxial strain	
	E_{11}	D_{11}	E_{11}	D_{11}
0.7	-0.106	-0.134	-0.255	-0.520
0.8	-0.069	-0.080	-0.180	-0.281
0.9	-0.034	-0.036	-0.095	-0.117
1.0	0.000	0.000	0.000	0.000
1.1	+0.033	+0.031	+0.105	+0.087

three are difficult to measure very accurately in experiments [Thurston, 1974], and those of orders four and higher are even more difficult to obtain and have been reported for very few crystalline solids.

While such benefits of Eulerian theory are readily apparent for loading conditions relevant to shock compression and hydrostatic compression, the same assertions do not necessarily hold for other loading protocols. In tension, for example, Lagrangian strain components increase more rapidly than Eulerian components (Table 5), opposite to what occurs in compression, leading to different trends in predicted material response. However, most crystalline metallic samples of significant size will undergo cavitation or tensile fracture when subjected to finite tensile volumetric strain, and they will undergo plastic slip, twinning, or shear fracture when subjected to large deviatoric strain. Thus, effects of choice of Lagrangian versus Eulerian theory become of low significance since large *elastic* tensile or deviatoric deformations are not sustainable. On the other hand, in other material classes such as rubber and ductile polymers, large elastic tensile and/or shear deformations are often sustainable, and nonlinear elastic potentials (neo-Hookean, Mooney-Rivlin, etc.) that may differ significantly from the present Lagrangian or Eulerian Taylor-type polynomials have been successful for describing their responses, often isotropic and/or (nearly) incompressible [Ogden, 1984]. Large elastic deviatoric strains may also be possible in some molecular crystals [Clayton and Becker, 2012] or in other crystalline nonmetals with restricted slip systems, especially under conditions where confining pressures are large enough to suppress fracture, for example indentation.

5. Conclusions

The response of metallic solids to planar shock loading has been analyzed in the context of nonlinear Lagrangian and Eulerian thermoelasticity models, the latter incorporating a relatively uncommon “Eulerian” strain referred to material coordinates. Predictions of shock stress for Eulerian and Lagrangian theories have been compared for several anisotropic metallic single crystals (Al, Cu and Mg), with elastic constants of up to order four included. Differences between predictions of each model as the number of higher-order constants is increased are smaller for Eulerian theory than Lagrangian theory, and higher-order constants themselves are of smaller magnitude for Eulerian than Lagrangian theory, suggesting greater accuracy and faster convergence of Eulerian over Lagrangian theory. Eulerian theory also more closely matches atomic simulation data for elastic shock compression of aluminum.

A continuum crystal plasticity framework has been developed that incorporates an Eulerian elastic strain tensor in the thermodynamic potentials. The fundamental difference between this framework and traditional Lagrangian crystal elastoplasticity in the resulting thermodynamic relations is the different constitutive equality for stress, which can result in different driving forces for slip (i.e., critical resolved shear stresses) and different pressure–volume behavior when internal energy potentials are truncated at finite order. Differences in critical resolved shear stresses derived for

the two third-order elastic models have been shown to become important at volumetric compressions in excess of about one percent. Different values of resolved shear stress would be obtained from the two different models from axial shock Hugoniot data for materials with Hugoniot elastic limits in excess of several percent of their bulk modulus, an important consideration for deducing dynamic strengths of strong solids. At shock pressures above the HEL in polycrystalline Al, Cu and Mg, Eulerian theory provides a better fit to experimental shock compression data than Lagrangian theory of the same order. The analysis empirically suggests that this Eulerian theory is preferable to traditional Lagrangian theory for modeling the shock response of these metals.

Appendix: Elastic Potentials, Elastic Constants, and Equations-of-State

Consider Taylor polynomial expansions of Lagrangian and Eulerian internal energy functions in (2.5) of order three in respective strain measures \mathbf{E} and \mathbf{D} , restricted here to isentropic conditions (i.e., omitting η dependence) for illustrative simplicity

$$\bar{U}(\mathbf{E}) = \frac{1}{2}\bar{C}_{IJKL}E_{IJ}E_{KL} + \frac{1}{6}\bar{C}_{IJKLMNOP}E_{IJ}E_{KL}E_{MN} + O(\|\mathbf{E}\|^4), \quad (\text{A.1})$$

$$\hat{U}(\mathbf{D}) = \frac{1}{2}\hat{C}_{IJKL}D_{IJ}D_{KL} + \frac{1}{6}\hat{C}_{IJKLMNOP}D_{IJ}D_{KL}D_{MN} + O(\|\mathbf{D}\|^4). \quad (\text{A.2})$$

Terms linear in either strain measure vanish by presuming that the unstrained reference state is stress free, and strain energy is also assumed to vanish in this unstrained reference state. The following kinematic identities apply:

$$\begin{aligned} \partial E_{IJ}/\partial F_{kL} &= \frac{1}{2}(\delta_{IL}F_{kJ} + \delta_{JL}F_{ki}), \\ \partial D_{IJ}/\partial F_{kL} &= \frac{1}{2}F_{Lm}^{-1}(F_{Ik}^{-1}F_{Jm}^{-1} + F_{Jk}^{-1}F_{Im}^{-1}). \end{aligned} \quad (\text{A.3})$$

Chain rule differentiation and use of (2.6), (2.7) and (A.3) then lead to

$$\frac{\partial^2 \bar{U}}{\partial F_{iJ} \partial F_{kL}} = F_{iN} F_{kM} \frac{\partial^2 \bar{U}}{\partial E_{JN} \partial E_{LM}} + \delta_{ik} F_{Jn}^{-1} P_{nL}, \quad (P_{iJ} = J F_{Jk}^{-1} \sigma_{ik}), \quad (\text{A.4})$$

$$\begin{aligned} \frac{\partial^2 \hat{U}}{\partial F_{iJ} \partial F_{kL}} &= F_{Qi}^{-1} F_{Ik}^{-1} F_{Jm}^{-1} F_{Rm}^{-1} F_{Ln}^{-1} F_{Pn}^{-1} \frac{\partial^2 \hat{U}}{\partial D_{QR} \partial D_{IP}} \\ &\quad - F_{Jk}^{-1} P_{iL} - F_{Li}^{-1} P_{kJ} - F_{Jm}^{-1} F_{Lm}^{-1} F_{kN} P_{iN}, \end{aligned} \quad (\text{A.5})$$

with \mathbf{P} the first Piola–Kirchhoff stress. In the undeformed, stress free reference state, (A.4) and (A.5) reduce to

$$\left(\frac{\partial^2 \bar{U}}{\partial F_{iJ} \partial F_{kL}} \right) \Big|_{\mathbf{F}=1} = \delta_{iM} \delta_{kN} \bar{C}_{MJNL}, \quad \left(\frac{\partial^2 \hat{U}}{\partial F_{iJ} \partial F_{kL}} \right) \Big|_{\mathbf{F}=1} = \delta_{iM} \delta_{kN} \hat{C}_{MJNL}. \quad (\text{A.6})$$

Assuming that second-order tangent moduli (second derivatives of internal energy with respect to \mathbf{F}) are equal at the reference state by equating left-hand sides of each of (A.6), it follows that second-order elastic constants are equivalent in Lagrangian and Eulerian theories (Voigt indices in Greek)

$$\bar{\mathbf{C}}_{IJKL} = \hat{\mathbf{C}}_{IJKL} = \mathbf{C}_{IJKL}, \quad \bar{C}_{\alpha\beta} = \hat{C}_{\alpha\beta} = C_{\alpha\beta}. \quad (\text{A.7})$$

Extending the same procedure by differentiating once further with respect to \mathbf{F} and equating third-order moduli $\partial^3 U / \partial \mathbf{F} \partial \mathbf{F} \partial \mathbf{F}$ for Lagrangian and Eulerian representations in the stress free reference state, third-order elastic constants are related by [Clayton, 2013]

$$\begin{aligned} \hat{\mathbf{C}}_{IJKLMN} = & \bar{\mathbf{C}}_{IJKLMN} + \delta_{IK} \mathbf{C}_{JLMN} + \delta_{IL} \mathbf{C}_{JKMN} \\ & + \delta_{IM} \mathbf{C}_{KLJN} + \delta_{IN} \mathbf{C}_{KLJM} + \delta_{JK} \mathbf{C}_{ILMN} \\ & + \delta_{JM} \mathbf{C}_{INKL} + \delta_{JL} \mathbf{C}_{IKMN} + \delta_{JN} \mathbf{C}_{IMKL} \\ & + \delta_{KM} \mathbf{C}_{IJLN} + \delta_{KN} \mathbf{C}_{IJLM} \\ & + \delta_{LM} \mathbf{C}_{IJKN} + \delta_{LN} \mathbf{C}_{IJKM}. \end{aligned} \quad (\text{A.8})$$

Extending this procedure to fourth order results in (2.25) for the uniaxial strain case. The second of (2.14) is derived by including polynomial terms in entropy change in internal energy functions (A.1) and (A.2) and equating cross-derivatives of internal energies with respect to \mathbf{F} and η [Clayton, 2013]. Note that (A.7) is consistent with the requirement that when strains are small enough, the difference between \mathbf{E} and \mathbf{D} becomes negligible (both approach the strain tensor of linear elasticity), and the second-order elastic constants become identical to those used in linear elasticity. Result (A.8) is consistent with the relationship derived elsewhere [Perrin and Delannoy, 1978] by substituting

$$\mathbf{D} = \mathbf{E} - 2\mathbf{E}^2 + 4\mathbf{E}^3 - \dots \approx \mathbf{E} - 2\mathbf{E}^2 \quad (\text{A.9})$$

into (A.2) and then equating terms of order three in \mathbf{E} in (A.1) and (A.2). Note that if the Eulerian strain energy potential (A.2) is exact at order three, for example, then the difference between internal energy functions (A.1) and (A.2) is the truncation error of the former, which is $O(\|\mathbf{E}\|^4)$. In other words, imposition of (A.7) and (A.8) does not ensure that (A.1) and (A.2) are equal since terms of orders four and higher in strain will lead to differences between the two energy functions that tend to become more pronounced at larger strain. However, if (A.1) and (A.2) are extended to polynomials of order n in strain, then truncation errors are of order $n + 1$ in some norms of strain tensors \mathbf{E} and \mathbf{D} ; these errors tend towards zero as $n \rightarrow \infty$ for regimes in which such norms are of less than unit magnitude, in which case (A.1) and (A.2) become both exact and equivalent.

For materials of high cubic or isotropic symmetry, the bulk modulus and its first derivative with respect to pressure, in the reference state, are, in Voigt notation

$$B_0 = \frac{1}{3}(C_{11} + 2C_{12}), \quad (\text{A.10})$$

$$B'_0 = -\frac{1}{3} \left(\frac{1}{3}\bar{C}_{111} + 2\bar{C}_{112} + \frac{2}{3}\bar{C}_{123} \right) / B_0 = -\frac{1}{3} \left(\frac{1}{3}\hat{C}_{111} + 2\hat{C}_{112} + \frac{2}{3}\hat{C}_{123} \right) / B_0 + 4. \quad (\text{A.11})$$

Derivations of the first of (A.11) can be found in Thurston [1965] and Teodosiu [1982]. The second equality of (A.11) then follows upon use of (A.8). Letting $\mathbf{F} = J^{1/3}\mathbf{1}$ in (A.1) and (A.2), and then applying stress–strain relations (2.6)₁ and (2.7)₁, Cauchy stress becomes of the spherical form $\boldsymbol{\sigma} = -p\mathbf{1}$, where the resulting pressures p corresponding to (A.1) and (A.2) are given by equations-of-state (2.8) and (2.9), respectively. Truncation errors, which are not written explicitly in these equations-of-state, are roughly of order three in corresponding strains since truncation errors in internal energy are of order four.

References

- Anand, L. [1979] “On H. Hencky’s approximate strain-energy function for moderate deformations,” *Journal of Applied Mechanics* **46**, 78–82.
- Asaro, R. J. [1983] “Crystal plasticity,” *Journal of Applied Mechanics* **50**, 921–934.
- Birch, F. [1947] “Finite elastic strain of cubic crystals,” *Physical Review* **71**, 809–824.
- Birch, F. [1978] “Finite strain isotherm and velocities for single-crystal and poly-crystalline NaCl at high pressures and 300°K,” *Journal of Geophysical Research* **83**, 1257–1268.
- Clayton, J. D. [2005] “Dynamic plasticity and fracture in high density polycrystals: Constitutive modeling and numerical simulation,” *Journal of the Mechanics and Physics of Solids* **53**, 261–301.
- Clayton, J. D. [2008] “A model for deformation and fragmentation in crushable brittle solids,” *International Journal of Impact Engineering* **35**, 269–289.
- Clayton, J. D. [2009] “A continuum description of nonlinear elasticity, slip and twinning, with application to sapphire,” *Proceedings of the Royal Society (London) A* **465**, 307–334.
- Clayton, J. D. [2010] “Modeling nonlinear electromechanical behavior of shocked silicon carbide,” *Journal of Applied Physics* **107**, 013520.
- Clayton, J. D. [2011] *Nonlinear Mechanics of Crystals* (Springer, Dordrecht).
- Clayton, J. D. [2012] “On anholonomic deformation, geometry, and differentiation,” *Mathematics and Mechanics of Solids* **17**, 702–735.
- Clayton, J. D. [2013] “Nonlinear Eulerian thermoelasticity for anisotropic crystals,” *Journal of the Mechanics and Physics of Solids* **61**, 1983–2014.
- Clayton, J. D. and Becker, R. [2012] “Elastic-plastic behavior of cyclotrimethylene trinitramine single crystals under spherical indentation: Modeling and simulation,” *Journal of Applied Physics* **111**, 063512.
- Clayton, J. D., Bammann, D. J. and McDowell, D. L. [2005] “A geometric framework for the kinematics of crystals with defects,” *Philosophical Magazine* **85**, 3983–4010.
- Clayton, J. D., Hartley, C. S. and McDowell, D. L. [2014] “The missing term in the decomposition of finite deformation,” *International Journal of Plasticity* **52**, 51–76.

- Clayton, J. D. and Knap, J. [2011] “A phase field model of deformation twinning: Nonlinear theory and numerical simulations,” *Physica D* **240**, 841–858.
- Clayton, J. D. and Knap, J. [2013] “Phase-field analysis of fracture-induced twinning in single crystals,” *Acta Materialia* **61**, 5341–5353.
- Davies, G. F. [1973] “Invariant finite strain measures in elasticity and lattice dynamics,” *Journal of the Physics and Chemistry of Solids* **34**, 841–845.
- Davies, G. F. [1974] “Effective elastic moduli under hydrostatic stress—I quasi-harmonic theory,” *Journal of the Physics and Chemistry of Solids* **35**, 1513–1520.
- Fouk, J. W. and Vogler, T. J. [2010] “A grain-scale study of spall in brittle materials,” *International Journal of Fracture* **173**, 225–242.
- Germain, P. and Lee, E. H. [1973] “On shock waves in elastic-plastic solids,” *Journal of the Mechanics and Physics of Solids* **21**, 359–382.
- Graham, R. A. and Brooks, W. P. [1971] “Shock-wave compression of sapphire from 15 to 420 kbar: The effects of large anisotropic compressions,” *Journal of the Physics and Chemistry of Solids* **32**, 2311–2330.
- Greene, R. G., Luo, H. and Ruoff, A. L. [1994] “Al as a simple solid: High pressure study to 220 GPa (2.2 Mbar),” *Physical Review Letters* **73**, 2075–2078.
- Guinan, M. W. and Steinberg, D. J. [1974] “Pressure and temperature derivatives of the isotropic polycrystalline shear modulus for 65 elements,” *Journal of the Physics and Chemistry of Solids* **35**, 1501–1512.
- Hiki, Y. and Granato, A. V. [1966] “Anharmonicity in noble metals: Higher order elastic constants,” *Physical Review* **144**, 411–419.
- Jeanloz, R. [1989] “Shock wave equation of state and finite strain theory,” *Journal of Geophysical Research* **94**, 5873–5886.
- Johnson, J. N. [1972] “Calculation of plane-wave propagation in anisotropic elastic-plastic solids,” *Journal of Applied Physics* **43**, 2074–2082.
- Johnson, J. N. [1974] “Wave velocities in shock-compressed cubic and hexagonal single crystals above the elastic limit,” *Journal of the Physics and Chemistry of Solids* **35**, 609–616.
- Johnson, J. N., Jones, O. E. and Michaels, T. E. [1970] “Dislocation dynamics and single-crystal constitutive relations: Shock-wave propagation and precursor decay,” *Journal of Applied Physics* **41**, 2330–2339.
- Lang, J. M. and Gupta, Y. M. [2010] “Strength and elastic deformation of natural and synthetic diamond crystals shock compressed along [100],” *Journal of Applied Physics* **107**, 113538.
- Luscher, D. J., Bronkhorst, C. A., Alleman, C. N. and Addessio, F. L. [2013] “A model for finite-deformation nonlinear thermomechanical response of single crystal copper under shock conditions,” *Journal of the Mechanics and Physics of Solids* **61**, 1877–1894.
- Mao, H. K., Bell, P. M., Shaner, J. W. and Steinberg, D. J. [1978] “Specific volume measurements of Cu, Mo, Pd and Ag and calibration of the ruby R_1 fluorescence pressure gauge from 0.06 to 1 Mbar,” *Journal of Applied Physics* **49**, 3276–3283.
- Marsh, S. P. [1980] *LASL Shock Hugoniot Data* (University of California Press, Berkeley).
- Murnaghan, F. D. [1937] “Finite deformations of an elastic solid,” *American Journal of Mathematics* **59**, 235–260.
- Naimon, E. R. [1971] “Third-order elastic constants of magnesium. I. experimental,” *Physical Review B* **4**, 4291–4296.
- Nielsen, O. H. [1986] “Optical phonons and elasticity of diamond at megabar stresses,” *Physical Review B* **34**, 5808–5819.
- Ogden, R. W. [1984] *Nonlinear Elastic Deformations* (Ellis Horwood, Chichester).

- Perrin, G. and Delannoy, M. [1978] "Application de la theorie des deformations finies a la determination de proprietes elastiques des polycristaux de symetrie hexagonale sous haute pression," *Journal de Physique* **39**, 1085–1095.
- Rao, R. R. and Padmaja, A. [1990] "Fourth-order elastic constants of nonideal HCP crystal Mg and Er," *Journal of Applied Physics* **67**, 227–229.
- Rice, J. R. [1971] "Inelastic constitutive relations for solids: An internal-variable theory and its application to metal plasticity," *Journal of the Mechanics and Physics of Solids* **19**, 433–455.
- Riedle, J., Gumbsch, P. and Fischmeister, H. F. [1996] "Cleavage anisotropy in tungsten single crystals," *Physical Review Letters* **76**, 3594–3597.
- Rosakis, P., Rosakis, A. J., Ravichandran, G. and Hodowany, J. [2000] "A thermodynamic internal variable model for the partition of plastic work into heat and stored energy in metals," *Journal of the Mechanics and Physics of Solids* **48**, 581–607.
- Slutsky, L. J. and Garland, C. W. [1957] "Elastic constants of magnesium from 4.2 K to 300 K," *Physical Review* **107**, 972–976.
- Teodosiu, C. [1982] *Elastic Models of Crystal Defects* (Springer, Berlin).
- Thomas, J. F. [1968] "Third-order elastic constants of aluminum," *Physical Review* **175**, 955–962.
- Thomsen, L. [1970] "On the fourth-order anharmonic equation of state of solids," *Journal of the Physics and Chemistry of Solids* **31**, 2003–2016.
- Thomsen, L. [1972] "The fourth-order anharmonic theory: Elasticity and stability," *Journal of the Physics and Chemistry of Solids* **33**, 363–378.
- Thurston, R. N. [1965] "Effective elastic coefficients for wave propagation in crystals under stress," *Journal of the Acoustical Society of America* **37**, 348–356.
- Thurston, R. N. [1974] "Waves in solids," in *Handbuch der Physik*, Vol. 4, ed. C. Truesdell (Springer, Berlin), pp. 109–308.
- Turneare, S. J. and Gupta, Y. M. [2011] "Material strength determination in the shock compressed state using X-ray diffraction measurements," *Journal of Applied Physics* **109**, 123510.
- Vogler, T. J. and Clayton, J. D. [2008] "Heterogeneous deformation and spall of an extruded tungsten alloy: Plate impact experiments and crystal plasticity modeling," *Journal of the Mechanics and Physics of Solids* **56**, 297–335.
- Wallace, D. C. [1972] *Thermodynamics of Crystals* (John Wiley & Sons, New York).
- Wallace, D. C. [1980] "Flow process of weak shocks in solids," *Physical Review B* **22**, 1487–1494.
- Wang, H. and Li, M. [2009] "Ab initio calculations of second, third, and fourth-order elastic constants for single crystals," *Physical Review B* **79**, 224102.
- Weaver, J. S. [1976] "Application of finite strain theory to non-cubic crystals," *Journal of the Physics and Chemistry of Solids* **37**, 711–718.
- Winey, J. M. and Gupta, Y. M. [2004] "Nonlinear anisotropic description for shocked single crystals: Thermoelastic response and pure mode wave propagation," *Journal of Applied Physics* **96**, 1993–1999.
- Winey, J. M. and Gupta, Y. M. [2006] "Nonlinear anisotropic description for the thermomechanical response of shocked single crystals: Inelastic deformation," *Journal of Applied Physics* **99**, 023510.
- Wu, P. D., Wang, H. and Neale, K. W. [2012] "On the large strain torsion of HCP polycrystals," *International Journal of Applied Mechanics* **4**, 1250024.
- Zimmerman, J. A., Winey, J. M. and Gupta, Y. M. [2011] "Elastic anisotropy of shocked aluminum single crystals: Use of molecular dynamics simulations," *Physical Review B* **83**, 184113.

1 DEFENSE TECHNICAL
(PDF) INFORMATION CTR
DTIC OCA

2 DIRECTOR
(PDF) US ARMY RESEARCH LAB
RDRL CIO LL
IMAL HRA MAIL & RECORDS MGMT

1 GOVT PRINTG OFC
(PDF) A MALHOTRA

37 DIR USARL
(PDF) RDRL CIH C
J KNAP
RDRL WM
B FORCH
J MCCAULEY
RDRL WML B
I BATYREV
B RICE
D TAYLOR
N WEINGARTEN
RDRL WML H
C MEYER
B SCHUSTER
RDRL WMM
J BEATTY
RDRL WMM B
G GAZONAS
D HOPKINS
B POWERS
C RANDOW
T SANO
RDRL WMM E
J SWAB
RDRL WMM F
M TSCHOPP
RDRL WMM G
J ANDZELM
RDRL WMP
S SCHOENFELD
RDRL WMP B
C HOPPEL
S SATAPATHY
M SCHEIDLER
A SOKOLOW
T WEERASOORIYA
RDRL WMP C
R BECKER
S BILYK
T BJERKE
D CASEM
J CLAYTON
D DANDEKAR
M GREENFIELD
R LEAVY

J LLOYD
S SEGLETES
A TONGE
C WILLIAMS
RDRL WMP D
R DONEY